OPEN ACCESS

Global Journal of Research in Engineering & Computer Sciences
ISSN: 2583-2727 (Online)
Volume 05| Issue 04 | July-Aug. | 2025
Journal homepage: https://gjrpublication.com/gjrecs/

Research Article

Radiotherapy Lung Cancer Advanced Treatment Planning Optimization for Fractionated Biological Effective Dose with Genetic Algorithm Pareto-Multiobjective Method. Third Part

*Francisco Casesnoves

PhD Engineering, MSc Physics-Mathematics, Physician. Bioengineering Laboratory Director. Independent Research Scientist. International Association of Advanced Materials, Sweden. UniScience Global Scientific Member, Wyoming, USA.

DOI: 10.5281/zenodo.16938699 **Submission Date:** 13 July 2025 | **Published Date:** 25 Aug. 2025

Corresponding author:** ***Francisco Casesnoves

PhD Engineering, MSc Physics-Mathematics, Physician. Bioengineering Laboratory Director. Independent Research Scientist. International Association of Advanced Materials, Sweden. UniScience Global Scientific Member, Wyoming, USA.

Email: *casesnoves.research.emailbox@gmail.com*

Abstract

This Third Part contribution constitutes an advance from previous articles in Breast and Head and Neck cancer Radiotherapy BED modelling (Biological Effective Dose). Lung tumors Hyperfractionation TPO (Treatment Planning Optimization) is programmed with Pareto-Multiobjective (PMO) Genetic Algorithms (GA) software. Artificial Intelligence methods (AI) with GA are applied on hyperfractionated TPO and detailed. Results comprise PMO-AI imaging process sequences and numerical values of PMO Lung cancer TPO parameters. Further results prove PMO-GA BED model both with Pareto-Optimal Front detailed graphics, charts, and numerical dose fractionation datasets. Solutions for improved and advanced RT Lung cancer TPO, and tumors in general for Fractional-dose photon dose delivery are explained. Mathematical Medical Physics analysis and a few review of lung tumor Isodoselines/Isodosezones, also numerical comparisons to previous published research for Breast Linear Quadratic Model and Head and Neck cancer PMO with Evolutionary Artificial Intelligence are briefed.

Keywords: *Pareto-Multiobjective Optimization (PMO), Mathematical Methods (MM), Biological Models (BM), Radiation Therapy (RT), Initial Tumor Clonogenes Number Population (N_0), Effective Tumor Population Clonogenes Number ($N_{Effective}$), Linear Quadratic Model (LQM), Integral Equation (IE), Tumor Control Probability (TCP), Normal Tissue Complications Probability (NTCP), Biological Effective model (BED), Tumor Control Cumulative Probability (TCCP), Radiation Photon-Dose (RPD), Nonlinear Optimization, Radiotherapy Treatment Planning Optimization (TPO), Source-Surface Distance (SSD), Software Engineering Methods, Radiation Photon-Dose, Attenuation Exponential Factor (AEF), Nonlinear Optimization, Radiotherapy Wedge Filter (WF), Anisotropic Analytic Model (AAA), Fluence Factor (FF), Omega Factor (OF), Treatment Planning Optimization (TPO), Breast Tumor (BT), Artificial Intelligence (AI), Pareto-Multiobjective Optimization (PMO), Genetic Algorithms (GA).*

Introduction And Objectives

Formerly, biological models BED-TPO simulations with AI-GA were proven in a series recent publications for Head and Neck and Breast tumors [75, 87-88, 91-96]. This article shows modelling advances from those methods/results towards one of the most epidemiologically frequent in male and female cancer patients actually, namely lung tumors. Artificial Intelligence with Genetic Algorithms in engineering software is applied on radiotherapy BED model for Lung cancer. The objective of this research is further development, programming, obtain two types of AI-GA 2D Graphics-numerical Optimization, and extensive dataset results for BED model hyper fractionated TPO protocol in Lung cancer [105]. Therefore, the focus of the study is getting accurate and software functionality optimization of BED model for lung cancer

hyper fractionated RT treatment. As an illustrative-introductory example, at Illustrative Examples 1-4, and Illustrative Table1 it is proven the utility of 3D imaging-processing of BED model for TPO. Isodoselines/Isodosezones were invented and developed in previous publications [105, Author's 1-4].

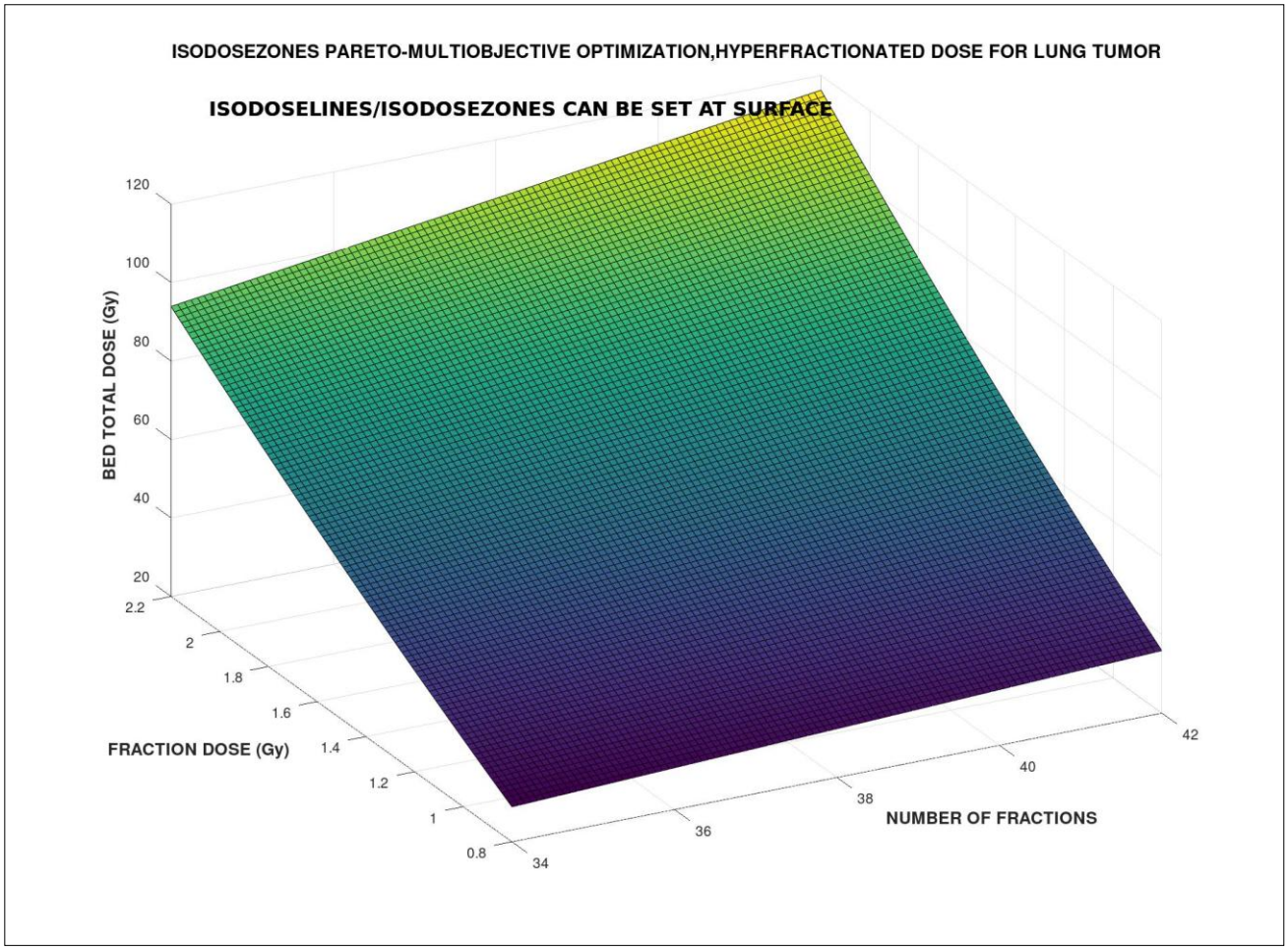

Illustrative Example 1.- From previous publications, [105, Author's 1-4], an implementation of BED model for lung tumors with GNU-Octave. Total dose standard is within [60,85] Gy and fraction magnitude can be selected from [0.8, 2.2] Gy. Number of fractions interval is [34,42]. With Matlab this 3D image-processing offers more numerical extraction possibilities. GNU-Octave image-processing quality is acceptable. The rest of parameters for BED model, (Algorithm 1.1), are presented in Tables 3-4.

This Third Part is focused mainly in 3D extended results and review of previous related publications, all together. Lung cancer Isodoselines/Isodosezones are briefed. Head and Neck cancer RT optimization results comparisons are shown. And a short part for Effective Clonogens modeling in breast tumor is commented. All of them present linked/related advances in Biological Models applications for RT treatment planning optimization. The tumor types selected, namely, lung, breast, and head and neck, are among the most frequent with higher incidence/prevalence worldwide.

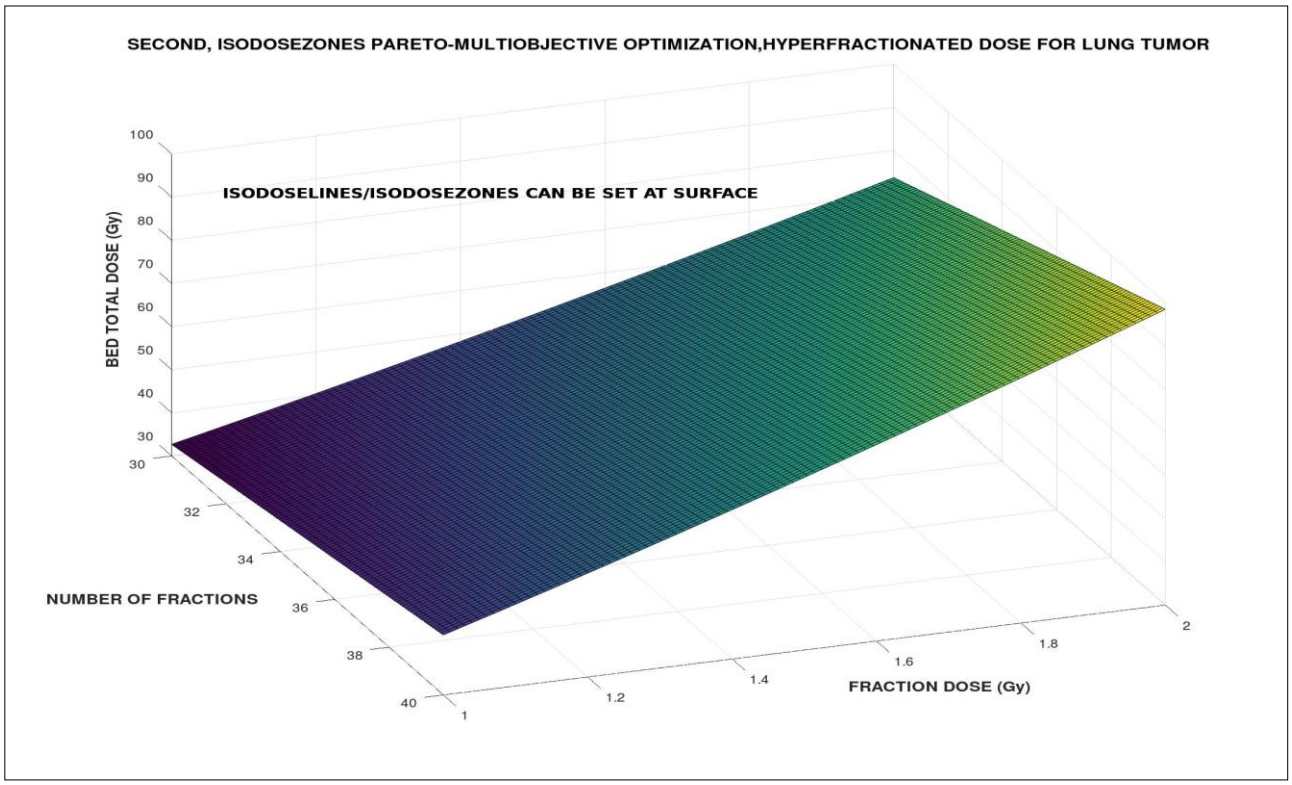

Illustrative Example 2.- From previous publications, [105, Author's 1-4], an implementation of BED model for lung tumors with GNU-Octave. On the left, total dose standard is within [60,85] Gy and fraction magnitude can be selected from [1.0, 2.0] Gy. Number of fractions interval is [30,40]. With Matlab this 3D image-processing offers more numerical extraction possibilities. GNU-Octave image-processing quality is acceptable. The rest of parameters for BED model,

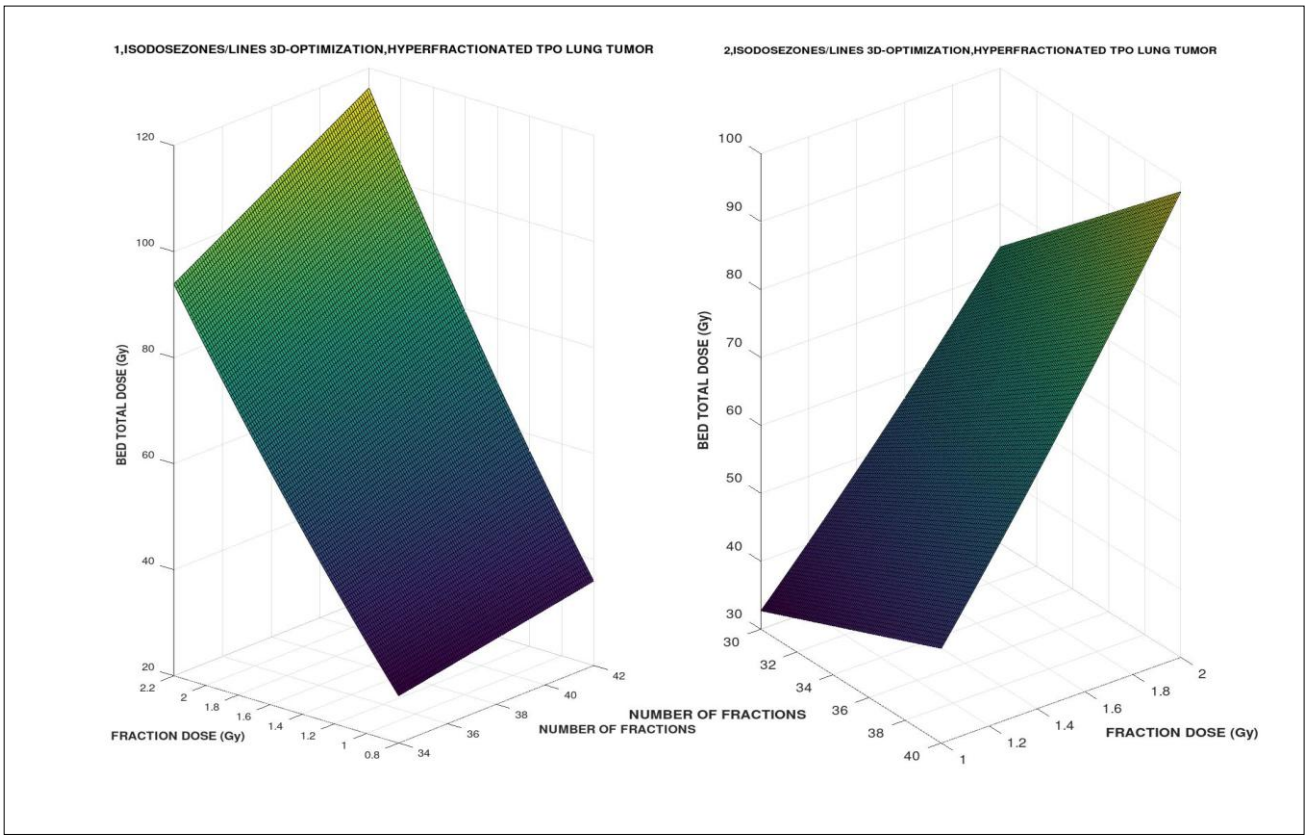

(Algorithm 1.1), are presented in Tables 3-4.

Illustrative Example 2.- GNU-Octave comparative 3D image-processing software. From previous publications, [105, Author's 1-4], an implementation of BED model for lung tumors with GNU-Octave. On the left, total dose standard is within [60,85] Gy, but increasing fraction number could reach 120 Gy, and fraction magnitude can be selected from [0.8, 2.2] Gy. Number of fractions interval is [34,42]. On the right, total dose standard is within [60,85] Gy, and could reach [90,100] GY, and fraction magnitude can be selected from [1.0, 2.0] Gy. Number of fractions interval is [30,40]. With Matlab this 3D image-processing offers more numerical extraction possibilities. GNU-Octave image-processing quality is acceptable. The rest of parameters for BED model, (Algorithm 1.1), are presented in Tables 3-4.

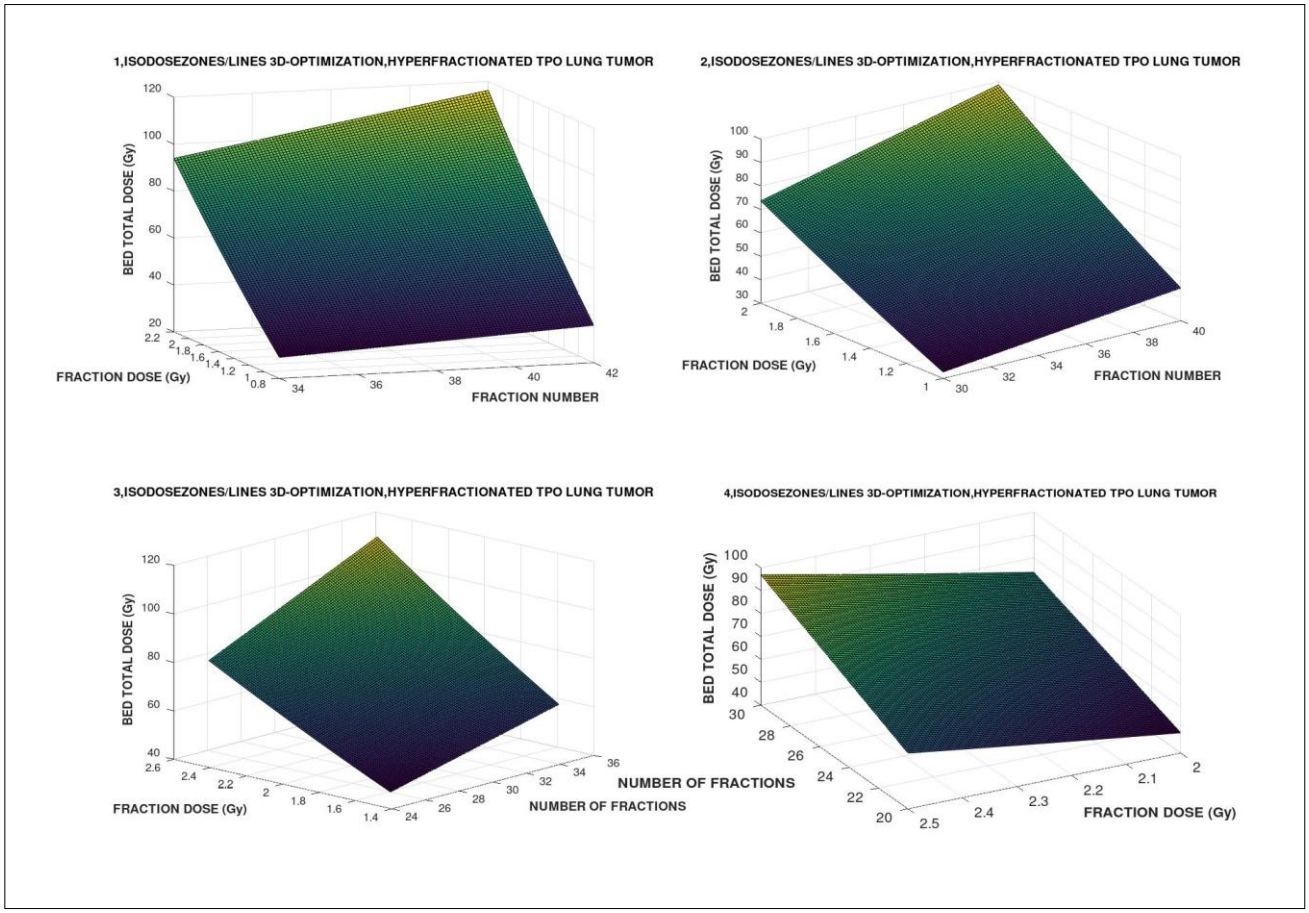

Illustrative Example 4.- Quadruple GNU-Octave simulation, from previous publications, [105, Author's 1-4], an implementation of BED model for lung tumors with GNU-Octave. (1). - Total dose standard is within [60,85] Gy, but could reach 120 Gy, fraction magnitude can be selected from [0.8, 2.2] Gy. Number of fractions interval is [34,42]. (2). - Total dose standard is within [60,85] Gy, but could reach 100 Gy, fraction magnitude can be selected from [1.0, 2.0] Gy. Number of fractions interval is [30,40]. (3). - Total dose standard is within [60,85] Gy, but could reach [100,120] Gy, fraction magnitude can be selected from [1.4, 2.6] Gy. Number of fractions interval is [24,36]. (4). - Total dose standard is within [60,85] Gy, but could reach [90,100] Gy, fraction magnitude can be selected from [2.0, 2.5] Gy. Number of fractions interval is [20,30]. Therefore, it is proven the efficacious applications for TPO of the 3D image-processing of BED model to select the most exact personal RT treatment at any patient. With Matlab this 3D image-processing offers more numerical extraction possibilities. GNU-Octave image-processing quality is acceptable. The rest of parameters for BED model, (Algorithm 1.1), are presented in Tables 3-4.

Epidemiologicaly, the importance of lung cancer screening among smokers and individuals with risk factors, has been proven recently. The reason is that survival rate after 5 years among early-stage diagnosed lung tumors is significantly higher [96, 106, 109, 111]. Surgical resection of lung tumors at stage I (T1–2, N0) NSCLC yields satisfying outcome results with 5-year survival rates of 60–70%, and remains at present the golden standard in this population. After resection, radiotherapy is optional.

Lung tumors are a heterogeneous type of cancer. Their incidence and prevalence are statisticaly among the highest percent of all tumors and constitute the highest deaths cancer rate at present. In general, [96], Non-Small-Cells-Lung carcinoma has a prevalence of approximately 85% of all lung tumors, while Small-Cells-Lung carcinoma shows about 15% of prevalence. In addition, lung and breast cancer show be the highest incidence in brain metastases [100]. For example, [90], 234,000 Primary Lung cancer cases in USA in 2018 with 154,050 deaths. In 1990 the incidence peak was [70 / 100,000 population], in 2018 [57 / 100,000 population]. This specific decrease of incidence in that developed country is probably due to healthier population habits related to tobacco consumption and contact with other toxic substances/chemicals. The most important oncological causal factor for lung cancer is proven be tobacco consumption, even in passive smokers. However, further pathogenesis factors are mainly chemical, from the external media intake/contact. Namely, radon gas, passive smoking, prior radiation from any radiation source [39-40,76-80], inhaled chemicals (polycyclic aromatic hydrocarbons), heavy metal inhaled particles and/or micro-nano particles. Among previous diseases, for instance pulmonary fibrosis. If any potential patient is smoker and at the same time is in contact with carcinogenetic chemicals, the oncogenetic synergism factor increases the probability of lung cancer. Therefore, although the tobacco consumption is decreasing in developed countries, it does not happen so in underdeveloped ones. This has caused an incidence/prevalence social-geographic-pathology rate displacement towards those countries. In addition, when smoking, the oral cavity can accumulate tobacco and alcohol as oncogenetical factors. This pathogenesis can cause concomitant diseases associated to the main lung tumor.

The radiosensitivity of tumor cells for optimal RT treatment has two main factors to be considered [82, 109], namely, alpha and betha coefficients and repopulation (Tumor Cells Intrinsic Radiosensitivity). From about 4 days after dose fraction irradiation, the fraction of clonogenes increases almost exponentially. Intrinsic radiosensivility is a crucial factor for Biological Effective Dose because the model depends on alpha and betha coefficients. The mathematical reason is that the exponential for survival fraction for radiobiological models is modified by these important parameters (Algorithm 2), [23]. According to [109], the alpha values vary [0.72, 0.52], and the betha one's change [0.047, 0.034], related to intermediate plating-delayed plating. In other words, RT schedule and patient personalized treatment for lung tumors should consider intrinsic radiosensitivity both for tumoral and normal tissues, when treatment planning optimization is calculated (NTCP, normal tissues complications probability and TCP, Tumor Control Probability constitute essential complementary probabilistic parameters when designing TPO).

The influence of oxygen model is a factor to be taken into account when using BED model. The main reason is the oxygenation factor on the numerical magnitude of alpha and betha parameters. A basic model is as follows, where, (α_o, β_o) and (α_h, β_h) are the radio sensitivities under oxygenated and hypoxic conditions respectively (Malinen et al. 2006):

$\alpha_h = \alpha_o / OER$ and $\beta_h = \beta_o / OER^2$

Where,

OER : oxygen enhancement ratio.

α_o : Alpha magnitude in oxygenation.

α_h : Alpha magnitude in hypoxygenation.

β_o : Betha magnitude in oxygenation.

β_h : Betha magnitude in hypoxygenation.

This distribution of hypoxia has also been used in previous modelling studies (Nahum et al. 2003; Wang et al. 2006), as a consequence the proportion of the total initial number of clonogens. This proportion is predicted by probability theory.

The influence of oxygen is linked to models of alpha and betha parameters related to the oxygen enhancement ratio (OER), whose formula is large and not set in the paper. The most important is:

If OER is higher than 1, alpha-hypoxia and betha-hypoxia decrease, then the Survival Fraction Equation negative exponential because alpha-oxygenated and betha-oxigenated increase. Therefore, in general, osygenated cells are more radiosensitive. Therefore, to get a survival fraction in oxygenated cells requires less radiation magnitude in general.

In brief, the α-hypoxia and β-hypoxia parameters for radiosenstitivity depend on PO_2, and this dependence can be described by the oxygen enhancement ratio (OER). In this classical oxygenation-radiosensitivity model the most important formulas are (Malinen et al. 2006):

$\alpha_h = \alpha_o / OER$ and $\beta_h = \beta_o / OER^2$

Where, (α_o, β_o) and (α_h, β_h) are the radiosensitivities under oxygenated and hypoxic conditions respectively.

Today, biomarkers are getting an important role in order to predict the survival time, optimal chemotherapy, and both characteristics at the same time [112]. Table 1 shows a biomarkers classification into P-Biomarkers (Biomarkers for Prognosis), T-Biomarkers (Biomarkers for Optimal Treatment), and H-Biomarkers (Hybrid Biomarkers Group), [Author's proposal]. General Biomarkers classification. Nano-Biomarkers is an open research field with potential perspectives in future [112]. Just remark that Biomarkers are is extent, diverse and difficult as involves biochemistry, molecular biology, medicine-pharmacology, medical physiology and several other fields. Therefore, this Table is simple based on Author's proposal classification. Hence, Biomarkers can be classified into two groups. Namely, T-Biomarkers, those specific for treatment, and P-biomarkers, those specific for prognosis, [Author's proposal, Table 1].

BIOMARKERS CLASSIFICATION FOR LUNG TUMOR RADIOTHERAPY TREATMENT
[Author's proposal]

BIOMARKER TYPE AND USAGE	CLINICAL APPLICATIONS	FUNCTIONALITY	RADIO-BIOCHEMICAL DETAILS AND RESEARCH
P-BIOMARKER (MAIN FUNCTION PROGNOSIS BIOMARKER)	Prediction of approximate survival time subject to optimal treatment . There are a large variety of techniques, for instance: Forward and Reverse Phase Protein Arrays, or Antibody and Antibody Detection–Based Assays [from 112]	Prediction for approximate survival based on specific tumor cell histology, and according to the relation histology-efficacy of drugs. Drug failure investigation utility.	The research in Biomarkers has experienced significant advances in recent years. Research clinical trial example, [from 112]: investigation data show that patient survival time in PD L1 positive patients who are treated with combined anti CTLA 4 and anti PD 1 is not superior to nivolumab monotherapy. That implied that was necessary further research. This clinical trial study area is difficult
T-BIOMARKER (MAIN FUNCTION TREATMENT BIOMARKER)	Selection of approximate optimal choice for treatment. Examples: dual-target recognition technologies.	Optimization of the best effective drug type for personalized tumor at every patient. Detection of optimal chemical-drug target and pharmacokinetics. Drug failure patient personalization investigation. Target characterization, or Dual target.	HSP90α is an inducible molecular chaperone that functions as a homodimer [ref 112, chapter 2.4, Table 2.4.2]. Research field involves physics, nuclear physics, biology, and chemistry.
H-BIOMARKER (HYBRID FUNCTION BIOMARKER)	Both prediction of survival time and optimal treatment	Specially those biomarkers that can make both functions, namely, prediction and treatment, or one of them better than the other.	Nano-Biomarkers actually in investigation can modify the inmuno cells and efficacy of chemical-drugs over cells tumor

Table 1.- Biomarkers Author's proposal of modern classification based on [101, 108, 109, 112].

In recent years, the TNM stage taxonomy was improved in the seventh edition of the staging guidelines to set a combination of TNM parameters with survival outcomes rates and treatment optimal choices among stages [refs]. Then, interrelated with TNM stages, mainly the survival rate, and prognosis rate, location, types of selected treatment strategies, divided into in stages I, II, III and IV are nowadays considered complementary. TNM classification has also defined survival rates for every stage. For example, T1a and IA show get the approximately equal survival rate after 5 years of about 50%. The interrelation of both criteria can be considered complex, since survival outcomes, surgery resection indication, RT treatment, chemotherapy and immunotherapy are linked to several stages of both taxonomies. For early stage: CT screening proven e useful. Low dose CT was proven be useful in screening. Screenings to get an early-stage diagnosis, and obtain an optimal treatment, are focused mainly on selected population smokers and high risk professions risk factors (such as toxic chemicals). TNM classification complemented with histologic grade is used today for precise diagnosis-stage of lung tumors. For example, TIa stage shows be the best survival rate after 5 years, 70%, while IV has a 10%. Pleural invasion, particularly the presence of tumor at the surface of the visceral pleura, has been an indicator of a poor prognosis.

Since radiotherapy treatment is indicated in all TNM lung cancer stages, it is possible to set a practical classification for specific lung tumor RT treatment, [author's proposal]. PTV Type 1 is a clinical planning for T and N stages located within thorax or very close into thorax to lungs. PTV Type 2 is the RT planning for N and M stages which are not close to primary lung tumor, such as, upper nodules at cervical-neck level, distant axile nodules or brain metastases.

Radiation therapy treatment is applied at all stages of lung cancer. Even at M stage, the brain metastases are treated with radiation, and when their diameter is about 5cm, radiosurgery is indicated [111]. Lung radiation has special anatomical and physiological constraints compared to other organs. Some of them are lung density inhomogeinity, which is a synergic difficulty with PTV volume changes with lung breath dynamics. During radiation delivery, the lung tumor target borders could vary about 2-3 cm [111], and at the same time that implied a dynamic density PTV change.

Radiotherapy biological models come from initial radiobiological theoretical and experimental studies [75, 87-88, 91]. Radiobiological interaction with normal tissues was researched for radioprotection [76-80]. Then, two practical branches emerged simultaneously from the equivalent mathematical modelling investigation. Namely, to use radiobiology knowledge for radiation protection of normal tissues, and conversely to set radiobiological models to approach/improve the cell-kill method in tumoral tissues [22-25, 89-91]. From this branch-duality, a practical swapping of equivalent parameters emerged for practical/easier research and clinical-biological applications. For instance [α, β] typical Linear Quadratic models parameters. These mathematical models both for normal and tumoral tissues were usually based on exponentials whose power-functions depend on a linear/nonlinear equation of radiation dose variable with a number of experimentally validated coefficients/constants [22-25, 76-80, 87- 91, 92-96].

The previous works and novelty in this artificial intelligence method for hyperfractionation precision-schedule method, [91,98,99,105], showed accurate results for survival fractions, 3D Graphical Optimization charts, and a database of numerical results in other type of cancer, e. g., prostate. To reach the research objectives in this study, nonlinear GA-PMO engineering software was programs for PMO-BED Lung cancer basic model. The implemented specific software got to get going towards improvements in GA programming and TPO radiotherapy optimization for BED model hyperfractionated dose delivery protocol [91].

Therefore, the innovation of this contribution shows a number of aspects. The first one is the application of Pareto-Multiobjective Optimization methods for lung cancer with in vivo dataset. The second one is the 3D Isodoselines in TPO with new imaging results, based on previous recognized publications [91, 98, 99, 105, 111]. The third is also the presentation of 3D Isodosezones improved imaging-processing results based on other recent article. Previous work with these methods belongs to prostate tumors and lung ones [91, 98, 99, 105, 111]. The primary algorithms and software results for these Pareto-Multiobjective Optimization were initially developed in these contributions.

Consequently, the innovation of this study is to carry out AI-GA programming for lung cancer hyperfractionation TPO in BED models. Several simulations with Genetic Algorithms are shown in 2D charts and numerical results. The algorithm for multiobjective pareto optimization is detailed and programmed. Results comprise GA simulations for two types of parameters-BED models according to literature [75, 87-88, 91]. Matlab system was used for GA programming with acceptable graphical processing images and numerical data findings.

Succinctly, advanced research from former Nonlinear Pareto-Multiobjective GA optimization was got for BED models in Lung cancer [87,88, 91]. Applications for radiotherapy TPO, dose delivery hyperfractionation schedule future biological model advances in modern RT are also presented.

Mathematical Algorithms and Software Engineering Methods

The model set in software patterns is the basic BED one [20-25,89]. There is a number of variations/simplifications of this model in the literature [20-25, 39,40,75, 85, 91]. One reason is that the radiobiological parameters determination vary according to experimental radiobiology data findings [20-25]. Therefore, those simplified BED models take statistical values of, for example, $T_{Potential}$ and others. In this section the algorithm is explained, at Results one, the Pareto-Multiobjective Optimization method parameters to put forward sharply the graphs are detailed.

Besides, in biological models TPO applications, there is a medical physics controversy/discussion about Hyperfractionation versus Hypofractionation dose TPO delivery. That point is beyond the scope of this study since the objective of the research is AI-GA optimization of hyperfractionation dose.

In this section the algorithms are explained, and at results one, the Pareto-Multiobjective Optimization method parameters to put forward sharply the graphs are detailed. However, for sharp learning, Table 2 shows the main simplified concepts of Genetic Algorithms applied on Pareto-Multiobjective Optimization.

It is very frequent the application of inverse least square techniques for RT inverse planning. Genetic algorithms constitute a more modern method, and GA Pareto-Multiobjective has also been applied recently [58, 67,110]. The genetic algorithms (GA) optimization method, closely linked to modern artificial intelligence, has experienced a recent increase in the use of its optimization applications/variants [58,67].

Although the applied GA method in this contribution is the standard, each one of the GA variants has its advantages and disadvantages [10,11]. Basically, GA is a stochastic mixed method similar to Monte Carlo but simpler/faster in general. That is, in plain language, successive generations of values (parameters) are computed by the software until the optimal parameters figures are obtained. Actually, the multiple combinations of random/stochastic methods, GA variants, and modern programming techniques, offer an extensive choice of options for the optimization designer. In this article, the parameters, namely, are, dose fraction magnitude, number of fractions, and total treatment time.

Therefore, here GA usually selects a randomly large number of successive generations of dose fractions number, fraction magnitude, and total treatment time, for the objective function maxima accuracy subject to constraints desired intervals for dose fractions number, fraction magnitude, and total treatment time. For every generation, three types of choices are applied for the OF. Namely, elite selection, after-mutations, and cross-over changes in the variables' values [110]. GA program stops when the number of generations subject to the constrains and/or the numerical tolerance for a generation is reached even if that solution is a local or global minimum. In other words, speaking roughly, GA stops when the best-possible and desired data for TPO that is needed is obtained.

SIMPLIFICATION OF GENETIC ALGORITHMS METHOD APPLIED TO PARETO-MULTIOBJECTIVE OPTIMIZATION		
PARAMETER	UTILITY	MATHEMATICAL SIGNIFICANCE
NUMBER OF GENERATIONS	To obtain the best results with the more efficacious generations number. The program is selecting the most accurate results (functions) after every generation, and discarding those (functions) whose errors are higher than constraints.	In general, the error decreases when reaching a prime number of generations, after that, the error differences are not significant
BEST FIT GENERATION	The program finally shows those generations (functions) that match the constraints better.	With Pareto-Multiobjective, the program shows two parameters at 2D chart: namely, best fit for pareto1 and best fit for pareto2
PARETO FRONT	The GA program works with two different functions, pareto1 and pareto2. That is presented in a 2D graph and the software-researcher can find the optimal points that satisfies better the objectives for both at the same mathematical parameters.	The most important when GA is applied on Multiobjective Optimization. Along the pareto front points given in 2D graph, the planner can select the best combination for both pareto function constraints.
DISTANCE AMONG INDIVIDUALS AND FITNESS OF EACH INDIVIDUAL	Along successive generations, they show how the individuals (values of pareto1 and pareto2) satisfy the constraints and algorithm. Then there are two parameters, accuracy for each and every individual independently, and comparative precision among individuals of every generation.	It gives the mathematical differences among successive generations. If it is not high, the meaning is that the method has got acceptable results.

Table 2.- Genetic Algorithms applied on Pareto-Multiobjective Optimization simple explanation.

Pareto-Multiobjective method is a specific optimization one, and here is implemented with GA. This method, for example, is extensively used also in economics to obtain optimal-comparative values for two options (actually 3 ones is

possible). Namely, Objective 1 and Objective 2. The method of multiobjective optimization for simple constraints begin with setting an objective function for the two different objectives with this type of functions:

$$\text{Minimize},$$
$$F(\vec{x}) = (f_1(\vec{x}), f_2(\vec{x}), \ldots . f_N(\vec{x})),$$
$$\text{subject to},$$
$$K_i(\vec{x}) \geq 0 \text{ , for } i = 1, \ldots . . M$$

Where

F(x) : Main function to be optimized.

f_i (x) : Every function of same variables (x).

K_i (x) : Constraints functions such as in general N ≠ M.

(1)

Algorithm 1.- The basic concepts of constrained Multiobjective Optimization.

Then, two alternatives (in paper total dose 50-55 Gy for Pareto1, and 60-65 for Pareto2, and for second simulation, table 2, 60 Gy Pareto1 and 65 Gy Pareto2, table 2, see all tables 1 and 2) are set within a built OF such as,

First Step Get the Bed Model as It Was Done for Head and Neck Cancer in Previous Publications:

$$\text{Chebyshev } L_1 \text{ Optimization for,}$$
$$BED_{Effective} = k\,d\left[1 + \frac{d \times \beta}{\alpha}\right] - \ldots$$
$$\ldots - \frac{Ln(2)}{\alpha}\left[\frac{T_{Treatment} - T_{Delay}}{T_{Potential}}\right];$$

(1)

where

k : Dose fraction number for hyperfractionated RT protocol. [20-25] .
Software pattern set [35 , 45] Fractions.
d : Dose fraction for hyperfractionated RT protocol. [20-25] .
Software pattern set [1 , 2.2] Gy.
α : Clonogen Head and Neck tumor radiosensitivity parameter [0.19 , 0.61]. [20-25] .
β : Clonogen Head and Neck tumor radiosensitivity parameter [0.0581] . [20-25] .
$T_{Treatment}$: Total time for radiation dose delivered.
Software pattern set [22 , 55] days. [20-25] .
T_{Delay} : Total standard repopulation delays for RT.
Software set [21] days. [20-25] .
$T_{Potential}$: Total standard Head and Neck cancer potential repopulation factor.
Software pattern set [3.5 , 4.5] days. [20-25] .

Algorithm (1.1)

Second Step: Setting This Model in L1 Objective Function:

Therefore, the Pareto-Multiobjective Optimization basic $BED_{Effective}$ created in this contribution algorithm-model was set in software, [91]. Parameters are detailed in Algorithm 1 [85-91]. Two different PMO optimization programming series are presented with different parameter intervals magnitudes, Tables 1-2. This BED model constitutes the fundamentals for fractionate radiotherapy, although there are variations among authors [22-25]. Formulation is based on previous studies computational software [1-21,85-91]. The algorithm that was set, with Chebyshev L_1 norm, [Algorithm 1], reads,

$$\text{Chebyshev} \quad L_1 \text{ Optimization,}$$

$$\text{for} \quad i = 1,2 \ldots \text{minimize pareto,}$$

$$\left| DOSE_i - BED_{Effective} \right|_{L_1} \text{ with,}$$

$$BED_{Effective} = k \times d \times \left[1 + \frac{d \times \beta}{\alpha} \right] - \ldots$$

$$\ldots - \frac{Ln(2)}{\alpha} \times \left[\frac{T_{Treatment} - T_{Delay}}{T_{Potential}} \right];$$

(Akgorithm 2)

Where,

BED: The basic algorithm for Biological Effective Dose initially developed by Fowler et Al. [22-25, 89].
K: Optimal Number of fractions for hyperfractionated TPO. Optimization parameter. [22-25, 89].
D: Optimal Dose magnitude for every fraction. Optimization Parameter [Gy]. [22-25, 89].
A: The basic algorithm constant for Biological Effective Dose models. Radiobiological experimental parameter. [Gy^{-1}]. [22-25, 89].
B: The basic algorithm constant for Biological Effective Dose models. Radiobiological experimental parameter. [Gy^{-2}]. It is very usual to set in biological models [α / β in Gy].
$T_{Treatment}$: The overall TPO time. This parameter varies according to authors' and institutions/hospitals criteria. [22-25, 89].
T_{Delay}: The overall TPO time delay for clonogens re-activation. This parameter varies according to authors' experimental research.

$T_{Potential}$: The potential time delay for tumor cell duplication. This parameter varies according to authors' experimental-theoretical research.

DOSE: The dose magnitudes for lung cancer simulation algorithm for Biological Effective Dose [22-25, 89]. Software patterns were calculated around intervals lung DOSE ϵ [50, 65] Gy.

Algorithm 2.- Lung cancer PMO algorithm [1-21,85-88] set in software loops, patterns, and arrays for AI-GA. The parameters interval-magnitudes for optimization are detailed in Tables 1-2. It is an improvement from a series of previous research in radiotherapy PMO-AI for Breast and Head and Neck tumors [75,87-88,91].

Pareto-Multiobjective Dataset for Lung Cancer Optimization

In the following, Table 2 shows the first simulation series according to data from [89]. Table 3 details dataset for second simulations series with experimental-theoretical magnitudes from [22-25]. In programming task, several trials around these values were done.

GENETIC ALGORITHM ARTIFICIAL INTELLIGENCE OPTIMIZATION PARAMETER INTERVAL FOR LUNG TUMORS FIRST OPTIMIZATION		
PARAMETERS WITH PROGRAMMING INTERVALS [First optimization with [ref 89] criterion]	MAGNITUDE INTERVAL	ADDITIONAL
Dose fractions number	Several trials [30, 40], [27, 32]	Schedule in literature [1-22-25,74-89,91, references for all this column].
Dose fraction magnitude	Several trials [1.5, 2.5], [1.3, 1.7], Gy	Schedule in literature. Set with intervals according to [89] criteria.
$T_{Treatment}$	Several trials [25,36], [30,40] Days	Schedule in literature. Set with intervals according to [89] criteria. The RT treatment [22-25] varies according to weekends, vacations, secondary effects in patient, circumstances, etc.
T_{Delay}	[15,20] Different from second simulation series	Schedule in literature. Set with intervals according to [89] criteria.
$T_{Potential}$ [programming interval]	[4.5, 5.5] At model denominator and different from second simulation series	Schedule in literature. Set with intervals according to [89] criteria.
Dose interval in Objective Function	50-55 Gy for Pareto function 1 60-65 Gy for Pareto function 2	Schedule in literature. Set with two total dose Pareto Functions according to [87-89, 91] different criteria.
α	[0.1, 0.6] Gy^{-1}	From [89]
β	0.035 Gy^{-2} Different from second simulations	From [89]

Table 3.-The first series simulations were done with approximate numerical-experimental data from several authors, mainly [89]. These parameter intervals are different from second series simulations.

GENETIC ALGORITHM ARTIFICIAL INTELLIGENCE OPTIMIZATION PARAMETER INTERVAL FOR LUNG TUMORS SECOND OPTIMIZATION		
PARAMETER [Second optimization with [refs 22-25,83] and related author's radiotherapy text books] criteria]	MAGNITUDE INTERVAL	ADDITIONAL
Dose fraction number	[25, 35] and [20, 30]	Schedule in literature [1-22-25,74-89,91-96, references applicable for all this column].
Dose fraction magnitude	[2.25, 3.25] Gy	Schedule in literature. Set with intervals according to [89] criteria.
$T_{Treatment}$	[30,32] Days	Schedule in literature. Set with intervals according to [22-25] criteria. The RT treatment [22-25] varies according to weekends, vacations, secondary effects in patient, circumstances, etc.
T_{Delay}	[21] Days standard	Schedule in literature. Set with intervals according to [22-25] criteria.
$T_{Potential}$ [programming interval]	[3.30, 4.10] Days	Schedule in literature. Set with intervals according to [22-25] criteria.
Dose interval in Objective Function	60 Gy for Pareto function 1 65 Gy for Pareto function 2	Schedule in literature. Set with two total dose Pareto Functions according to [87-89, 91] different criteria.
α	[0.1, 0.6] Gy^{-1}	From [22-25]
β	0.0581 Gy^{-2}	From [22-25]

Table 4.-The second series simulations were done with approximate numerical-experimental data from several authors, mainly [22-25]. These parameter intervals are different from first series simulations.

Results

Results are 2D AI-GA graphical and numerical. As shown in Table 2, the most important GA parameters are presented and explained. That is, Best Fit, Number of Generations and Pareto-Front. In Pareto-Front, the optimal point was selected to get the best results, Figure 1. Figures 6-7 show the histograms score data results, that is, the difference between the pareto1 and pareto2 scores.

For first simulations, Figures 1-4 show PMO results—Figure 3.1 is a variant of Figure 3. For the second group, 2D imaging processing are Figures 5-7. Tables 3-4 present details of both numerical PMO optimization results. The most important to validate the results are those ones that show the Pareto Front. Average distance among generation individuals, score histograms, stopping criteria, or fitness for every individual, are also significant. All the complementary details and shown in additional 2D charts for first and second AI-GA PMO optimization.

Maximum number of generations programmed is 300. Some other generations number to compare were selected as 100, General running time range for all images and both optimization trials is about 2-6 minutes. Numerical results, Tables 3-4, resume for PMO in BED model. Dose fraction magnitudes, number of fractions and optimal total RT treatment values are explained in Tables 3-4.

GA 2D RESULTS

First simulation 2D GA results are shown in Figures 1-4. The data for first and second simulation is set at Tables 3-4. Second one are presented in Figures 5-8. There are simple image processing charts and multifunctional images also. In Figure 1, the most important is the Pareto-Front first chart. Complementary, the Distance among individuals and the fitness of each individual is shown, concepts in Table 2.

First Simulation 2D Results

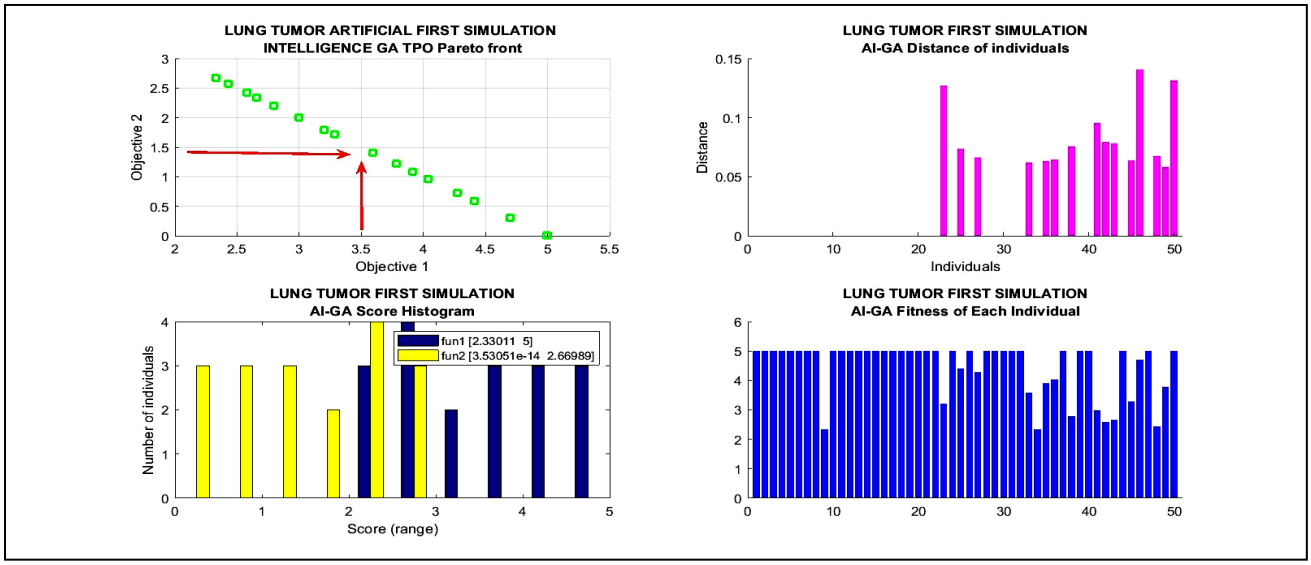

Figure 1.-First optimization Multifunctional AI-GA 2D graph. The Pareto-Front is the most important graph. When it shows low residuals the GA optimization is acceptable for Algorithm1. In this study both f 1 and f 2 show low 1.5 and 3.5 residuals. The number of points on the Pareto front was: 18. The number of generations is 300. Note the precision reached: pareto1 and pareto2 differ in approximately 1 Gy. Average distance among individuals is approximately lower than 0.5, and ftness of every individual is acceptable.

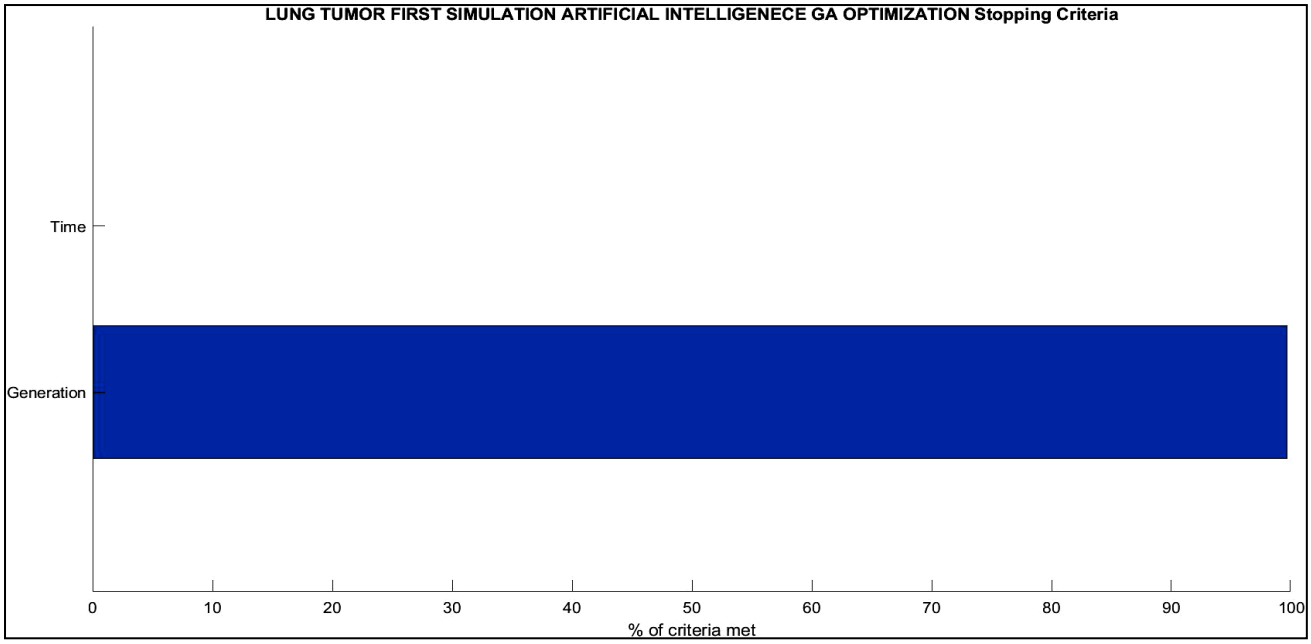

Figure 2.-Stopping criteria for first optimization showing 100% criteria met. At Y axis generation and time.

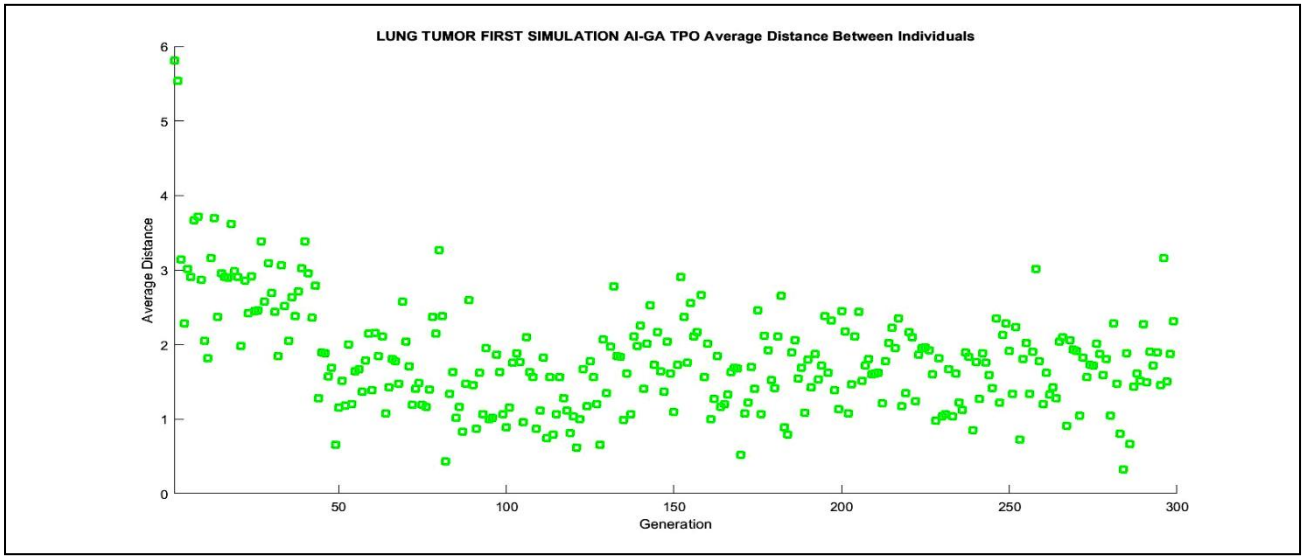

Figure 3.-This is a significant 2D GA graph. Most of average distance magnitude in lower than 2 from 50th generation on. The number of points on the Pareto front was: 18. The number of generations is 300.

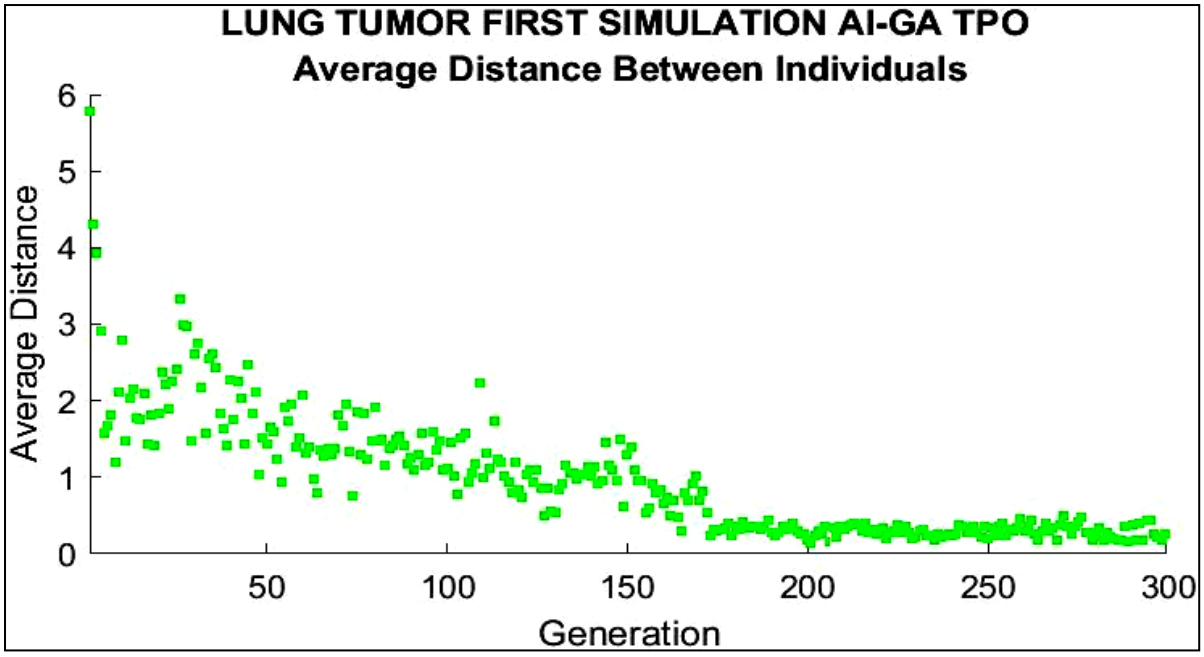

Figure 3.1.-Refinement of first optimization GA 2D graph from Figure 3. Average distance magnitude is approximately lower than 0.5 from 150th generation on.

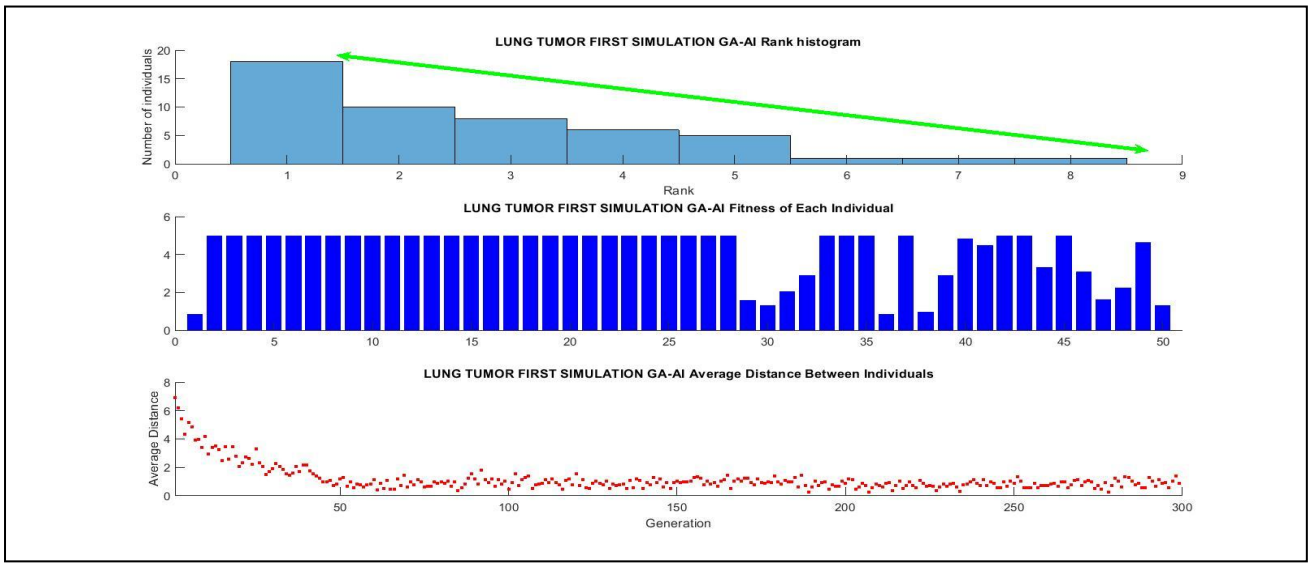

Figure 4.-First optimization Multifunctional GA 2D graph. It comprises rank histograms, note the error decreasing gradient. Fitness of each individual, inset, at second graph. Average distance at lowest image. All parameters show be precise, specially the rank histograms.

Second Simulation 2D Results

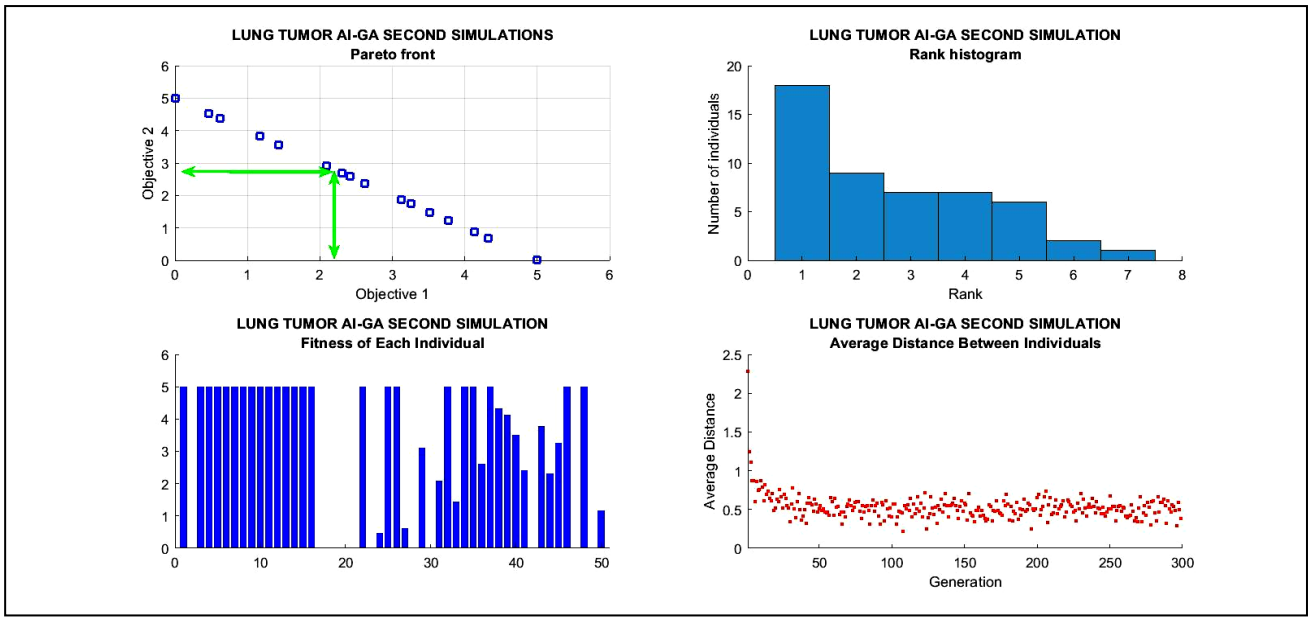

Figure 5.- Second optimization Multifunctional AI-GA 2D graph. The Pareto-Front is the most important graph. When it shows low residuals the GA optimization is acceptable for Algorithm1. In this study both f 1 and f 2 show lower than 3 residuals. The number of points on the Pareto front was: 18. The number of generations is 300. Average distance is lower than 1, about 0.5 from 50th generation on. One option for a balanced pareto-choice with approximate equal residuals for both pareto functions is marked inset with green arrows. In this second simulation pareto1 and pareto2 differences is lower than the first one.

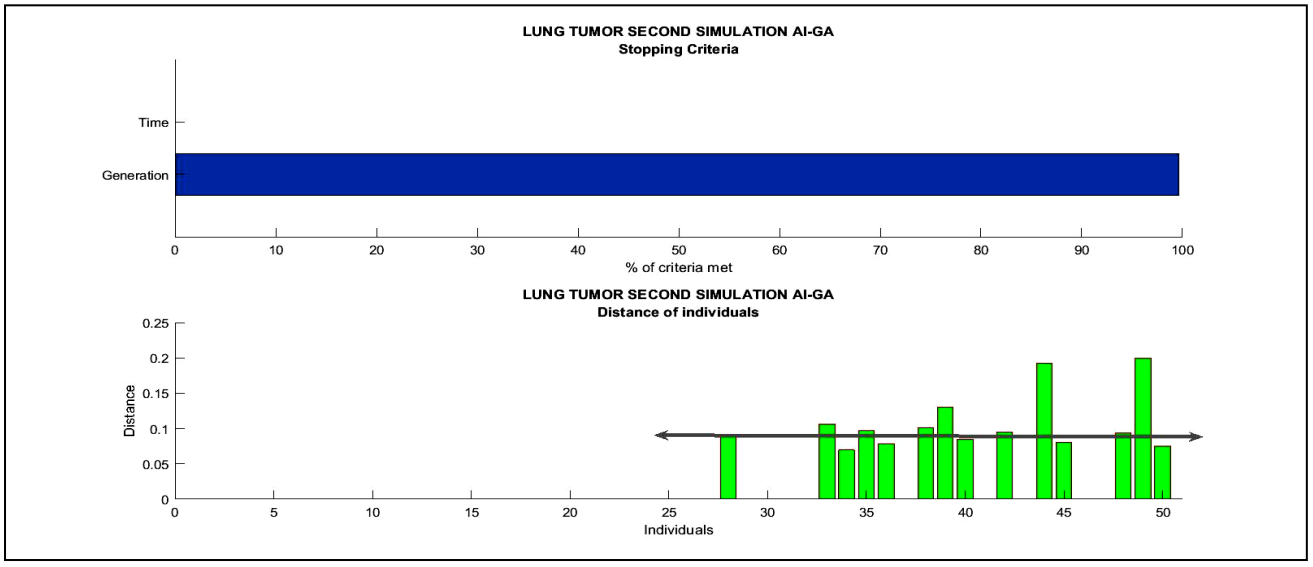

Figure 6.- Stopping criteria for second optimization showing 100% criteria met. At Y axis generation and time. Lower chart shows distance among individuals, in general lower than 0.1.

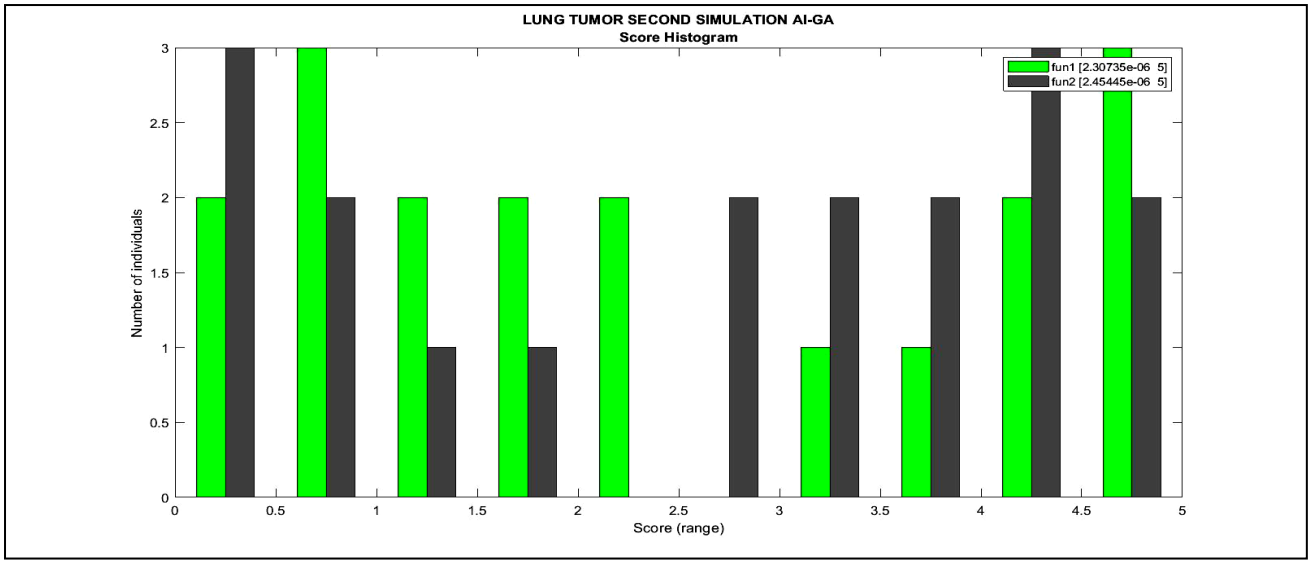

Figure 7.-Second optimization Score Histogram range.

GA Numerical Results

This section shows a brief of numerical dataset corresponding to imaging processing AI-GA results, Tables 4-5. It is useful to compare the dose per fraction and number of fractions among all optimal results.

First Simulation Numerical Results

The first simulation results are shown in Table 5. The second in Table 6. Main comparison should be among dose per fraction and number of fractions. Results are according to literature and recent advances [111] several hospital data.

GENETIC ALGORITHM ARTIFICIAL INTELLIGENCE OPTIMIZATION NUMERICAL RESULTS FOR LUNG TUMORS FIRST OPTIMIZATION		
PARAMETERS WITH PROGRAMMING INTERVALS [First optimization with [ref 89] criterion]	MAGNITUDE INTERVAL	ADDITIONAL
Dose optimal fraction number	[27, 31] Fractions	Usual protocol in literature [1-21,74-89].
Dose fraction optimal magnitude	[1.60, 1.90] Gy	Usual protocol in literature [1-21,74-89]. Set with intervals according to different criteria.
$T_{Treatment}$	[30,33] Days Different from second simulations	Usual protocol in literature [1-21,74-89]. Set with intervals according to different criteria. The RT treatment varies according to weekends breaks, secondary effects, patient circumstances, etc.
T_{Delay}	[12,16] Days From [89]	Usual protocol in literature [1-21,74-89]. Set with intervals according to different criteria.
$T_{Potential}$ [programming interval]	[4.5, 5.5] Different from second simulation series	Usual protocol in literature [1-21,74-89]. Set with intervals according to different criteria.
Dose interval in Objective Function	58 Gy for Pareto function 1 65 Gy for Pareto function 2	Usual protocol in literature [1-21,74-89]. Set with two total dose Pareto Functions according to different criteria.
α	[0.1, 0.6] Gy-1 Set in arrays [0.35 ± 0.25] Like second simulations	From [89]
β	0.035 Gy-2 Set in arrays	From [89]

Table 5.- PMO Artificial Intelligence with GA optimization first simulation series numerical results. Numerical results intervals, after several trials, match approximately [89] data.

Second Simulation Numerical Results

GENETIC ALGORITHM ARTIFICIAL INTELLIGENCE OPTIMIZATION NUMERICAL RESULTS FOR LUNG TUMORS SECOND OPTIMIZATION		
PARAMETER [Second optimization with [refs 25,83] and related author's radiotherapy text books criteria]	MAGNITUDE INTERVAL	ADDITIONAL
Dose fraction number	[19, 22]	Usual protocol in literature [1-21,74-86].
Dose fraction magnitude	[2.0, 2.5] Gy	Usual protocol in literature [1-21,74-86]. Set with intervals according to different criteria.
$T_{Treatment}$	[30,32] Days	Usual protocol in literature [1-21,74-86]. Set with intervals according to different criteria. The RT treatment varies according to weekends breaks, secondary effects, patient circumstances, etc.
T_{Delay}	[22,35] Days	Usual protocol in literature [1-21,74-86]. Set with intervals according to different criteria.
$T_{Potential}$ [programming interval]	[3.30, 4.10] Days	Usual protocol in literature [1-21,74-86]. Set with intervals according to different criteria.
Dose interval in Objective Function	60 Gy for Pareto F function 1 65 Gy for Pareto F function 2	Usual protocol in literature [1-21,74-86]. Set with two total dose Pareto Functions according to different criteria.
α	[0.1, 0.6] Gy^{-1}	From [25,83, and related authors' radiotherapy text books]
β	0.0581 Gy^{-2}	From [25,83, and related authors' radiotherapy text books]

Table 6.-Brief of PMO Artificial Intelligence with GA optimization second simulations series numerical results in Head and Neck tumors for advanced TPO. Dataset for software [22-25].

Previous Studies for Lung Cancer Isodoselines and Isodosezones, A Briefing

This section comprises the radiotherapy reminder of Isodoselines and Isodosezones from previous contributions, [Author's 1-2], Isodoselines and Isodosezones creation can be useful/practical in TPO when using BED or other models. For necessary understanding, Illustrative Examples 1-4, the following essential concepts are highlighted:

Definition 1.- In RT-3D Treatment Planning, a 3D Isodoseline is demarcated by a line whose dose-distribution parameters can vary for optimal planner choice while keeping constant the magnitude of total radiation dose delivered [Casesnoves, 2022].

Definition 2.- In RT-3D Treatment Planning, a 3D Isodosezone is demarcated by a polygon whose dose-distribution parameters can vary for optimal planner choice while keeping constant the total dose delivery magnitude [Casesnoves, 2022].

Some selected 3D image-processing Isodoselines and Isodosezones for TPO lung tumors, Figures 7.1 and 7.2 are,

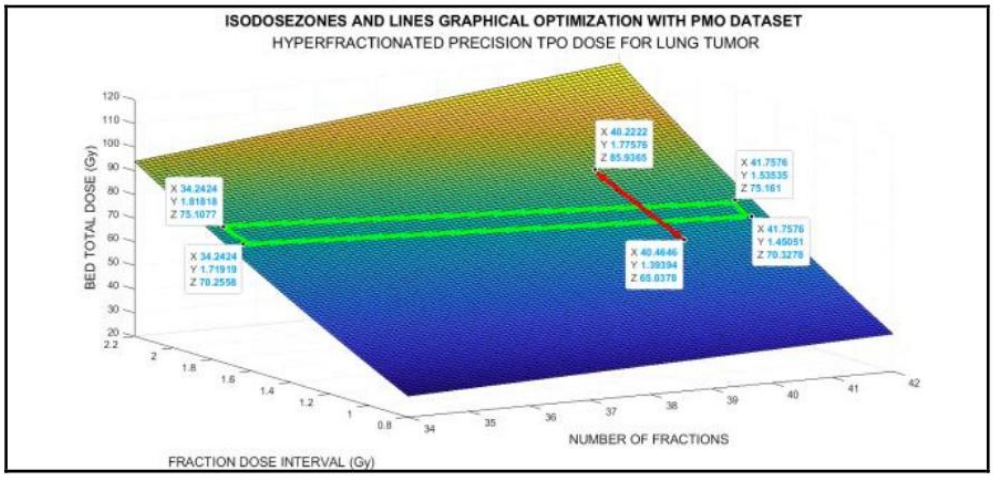

Figure 7.1.- From [Author's 1-2], Matlab 3D Isodosezone for two variables. Namely, the choice is number of fractions dose and total treatment dose in lung TPO. Namely, marked inset, [70,75] Gy isodosezone (green boundaries). Marked inset, [70,75] Gy isodosezone delimited by isodoselines. In literature, TPotential is usually set as 28-30 days for early stage lung cancer. Precision can be checked setting in Algorithm (1.1) at every extreme values of any long Isodosezone. Inset (red), and Isodoseline constrained to 40 fractions and for an interval of [65,85] Gy. The 3D Isodosezone fundamentals for Interior Optimization calculations, are implemented into this 3D surfactal isodosezone. Imaging-pattern numerical-intervals for plotting were obtained from PMO but with with in vivo lung tumor BED model parameters.

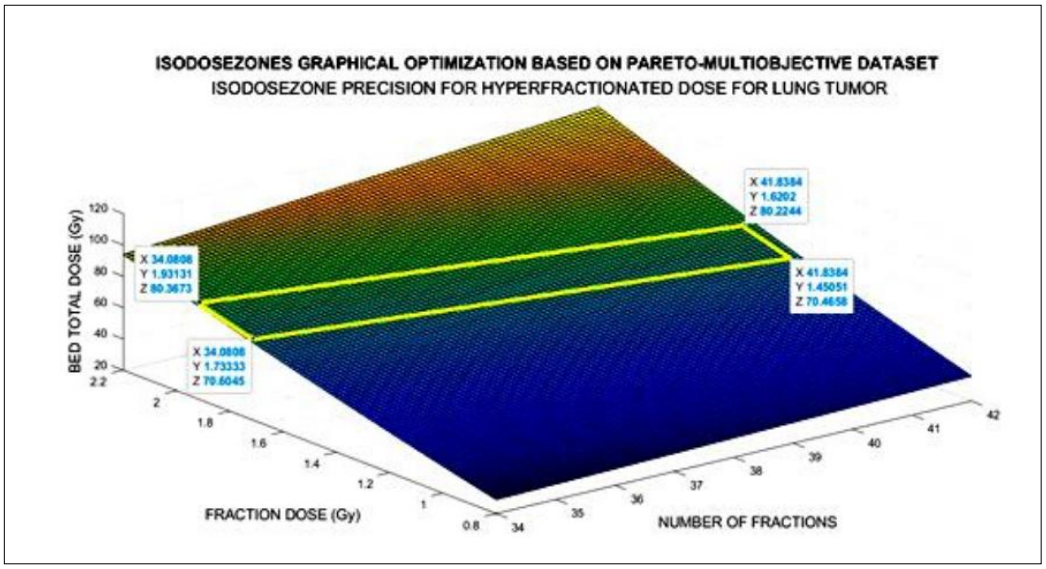

Figure 7.2. From [Author's 1-2], Matlab 3D Isodosezone for two variables, at XY plane, number of fractions and dose per fraction, the choice. Namely, Number of fractions and dose per fraction in lung TPO. Marked inset, [70,80] Gy isodosezone delimited by isodoselines. The precision can be checked calculating the product between fraction dose and number of fractions at each extreme of the long isodoselines. For instance, at lower isodoseline (yellow), 34 x 1.7 is approximately equal to 41 x 1.4 (taking one mdigit is exactly equal). The Isodosezone fundamentals from Interior Optimization calculations, are implemented into this 3D surface. The software-programming pattern intervals for plotting were taken from previous pareto multiobjective optimization developments but within vivo lung tumor BED parameters. Each and every BED total dose is set along 3D Isodoszone, while (k) and (d), and other BED model parameters change along the isodoselines-isodosezones surfactal length when cursor is moved over the surface.

Comparative Results with Head and Neck Cancer Computational Intelligence Ga Algorithm Optimization Research

Computational Intelligence GA comparison with the same method for Head and Neck tumors, Figures 8-9. These images included here are newly-developed different imaging processing PMO results than obtained in [87]. The most significant to check the results are the Pareto Front images, Figure 8. Figure 9 is a multifunctional image AI-GA processing for Head and Neck cancer RT treatment based on [87,91] software.

Distance among individuals, score histograms, and fitness of every individual are shown, Figure 9. Maximum number of generations selected was 300-800. Running time for Figure 8 is shorther than Figure 9, both processes is from 2 to 6 minutes.

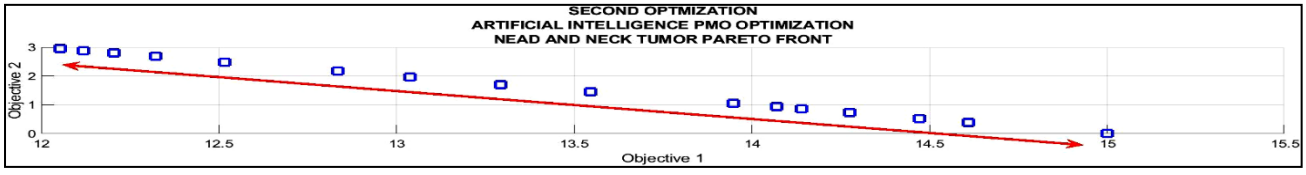

Figure 8.-This is the most pareto-multiobjective significant graph given by software when PMO is programmed. Note that Objective 2 shows be better than Objective 2 for Head and Neck tumors AI-GA optimization [87-88]. The number of points on the Pareto front was: 18. The number of generations is 300-800.

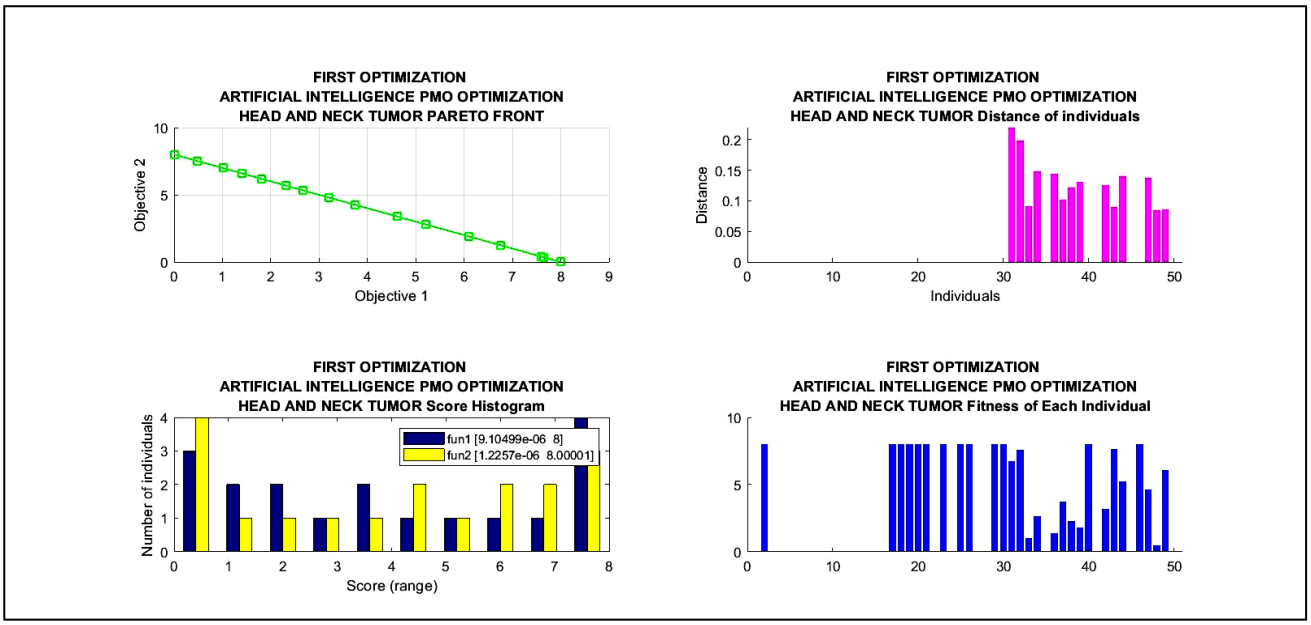

Figure 9.-Head and Neck tumors Pareto-Optimization Multifunctional GA 2D graph. Developed with software for [87-88]. It shows Distance among individuals, Fitness of every individual, and Score Histogram. Running time is about 3-4 minutes.

Comparative Results with Breast Cancer Effective Clonogens Model in Linear Quadratic Method, From Previous Contributions

From [Author's 3], a brief review in breast cancer. Radioprotection in radiotherapy and Environmental Radioprotection constitute a fundamental part to minimize and/or decrease the hazard ionizing radiation sources damage on the population. Breast cancer Radiation Protection for the patient during routinary RT treatment avoids multiple risk factors. Namely, RT overdose, OARs damage, increase of radiation use for high incidence/prevalence of breast cancer with subsequent RT oncology therapy, medical staff professional cumulative dose increase, hospital radiation contamination, environmental radiation contamination, and others.

Continuing the Radiation Therapy research studies series, this review of results study objective is the implementation of Tumor Clonogens Effective Population Number Model for breast cancer, [Fowler 1989- 2010] and [Author's 3]. Photon-dose AAA model former contributions result in breast tumors Biological Models (BM) TCP parameters, [From Author's 3, 1,74]. Development for 3D Graphical Optimization solutions from recent study to obtain Effective Tumor Clonogenes Survival Rate [$N_{Effective}$], constitutes the purpose of this research. Photon-beam Biological Models are based mainly on exponential functions with radiobiological parameters, namely [α, β], whose magnitudes are determined in general with in vitro experimental [From Author's 3, 19,21-24,74]. These parameters are implemented in BM to obtain Survival Fraction Clonogens Rate, [N_S]. N_S is function of [N_0], namely, initial clonogens population number. However, the innovation of this study determines the fitted to RT treatment time initial clonogens population number with the calculation of $N_{Effective}$ for breast cancer RT treatment. Table 7 shows basic results of [$N_{Effective}$] calculations for RT breast cancer.

Here I short review from [refs], is shown, to remark the clonogens population importance at Biological Models. The classical algorithm for $N_{Effective}$ clonogens population breast cancer, and in tumor generally, reads,

$$N_{Effective} = N_0 \times 2^{\left[\frac{(T - T_{Del})}{T_{Pot}}\right]};$$

Where,
$N_{Effective}$: Number of tumor clonogens in function of RT treatment protocol time.

N_0 : Initial Clonogens Number at starting RT time.

T : Total RT Treatment time.

T_{Delay} : Number of delay days after standard RT treatment time.

$T_{Potential}$: Potential Tumor Doubling Clonogens time.

Some example for results from [Author's, 3], are as follows,

NUMERICAL RESULTS FOR BED MODEL BREAST TUMORS RADIOTHERAPY PARETO-MULTIOBJECTIVE OPTIMIZATION [f_1 is optimized for 60 Gy, f_2 for 70 Gy]		
OPTIMAL FRACTIONS NUMBER	OPTIMAL FRACTION DOSE	OPTIMAL DAYS AFTER POTENTIAL TIME
[53 , 56]	[1.0572 ,1.1215] Gy	[24 ,29]

NUMERICAL RESULTS FOR $N_{Effective}$ MODEL BREAST TUMORS RADIOTHERAPY OPTIMIZATION				
Minimum $[N_0]$ Minimum $[T_{Delay}]$	Maximum $[N_0]$ Minimum $[T_{Delay}]$	Minimum $[N_{Effective}]$ Minimum $[T_{Delay}]$	Maximum $[N_0]$ Maximum $[T_{Delay}]$	Maximum $[N_{Effective}]$ Maximum $[T_{Delay}]$
1.01×10^2 1.18 days	1.00×10^{10} 1.18 days	1.06×10^{10} 1.18 days	1.00×10^{10} 19 days	2.562×10^{10} 19 days

Table 7.- From [Author's, 3], as an example, the clonogens Numerical results for $N_{effective}$ population and from [Author's, 3], the PMO for breast cancer.

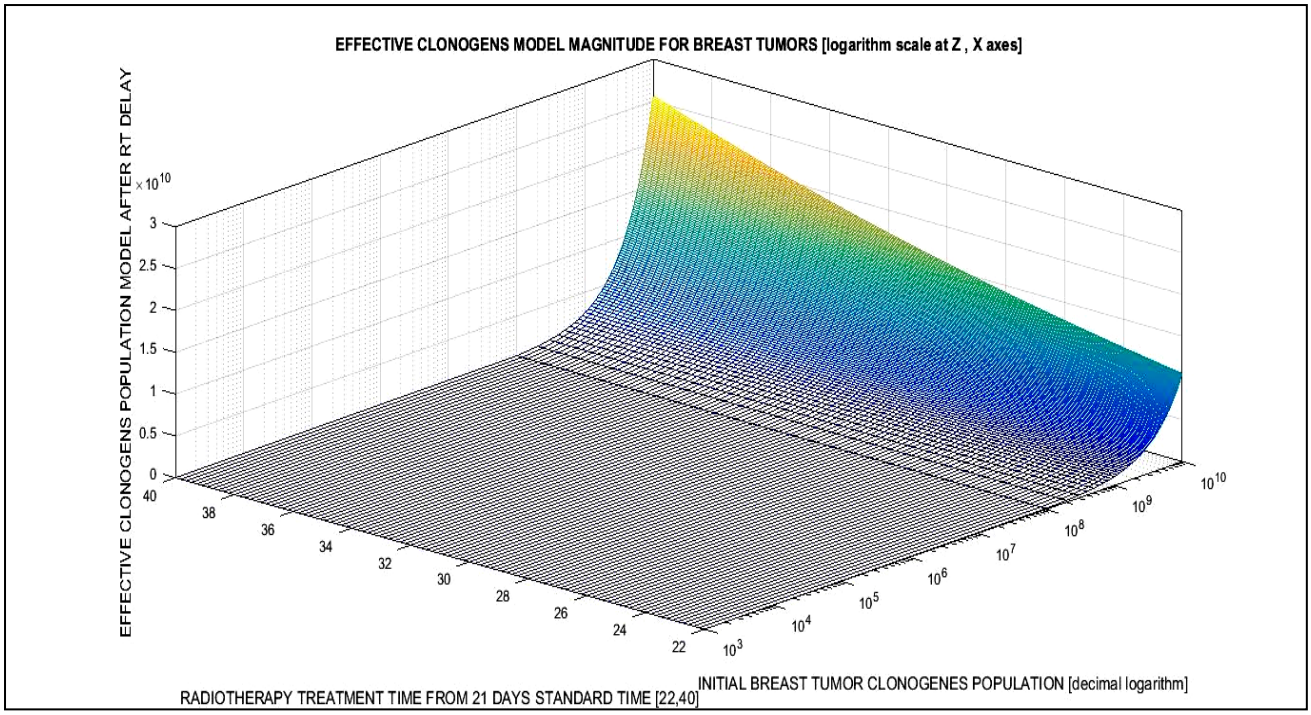

Figure 10.- From [Author's, 3], a 3D imaging processing graph for Effective clonogens population, (note logaritmic scale at Z, X axes). Observe the almost exponential growth from 10^8 logaritmic population magnitude, and also the same almost linear growth from 22 days to 40 days at Y axis.

Discussion and Conclusions

The objectives of the study were graphical and numerical optimization of standard BED model for modern Lung cancer TPO. The method applied was Artificial intelligence with GA Pareto-Multiobjective Optimization. It is the same technique from previous research with BED model for Breast and Head and Neck tumors TPO. Optimization was performed according to two authors' biological BED models criteria [22-25, 87-89,91]. Therefore, it constitutes a step forward to apply GA for Lung cancer TPO advances.

The mathematical method applied is Pareto-Multiobjective Optimization. The advantage of 2D Multiobjective Optimization compared to common one is to obtain at least two pareto functions, and the optimal choice can be got selecting the most convenient data from objective 1 and objective 2 graphs [Figs. 1,8,9]. Compared to Tikhonov Inverse Optimization method, that was applied in previous publications, that constitutes an advantage [21,75]. However, classical Tikhonov methods can be considered precise and useful. A useful-comprehensive simplification of the GA-PMO method was shown in Table 2. Complementary, and specifically for lung tumors, a Biomarkers Author's proposal of modern classification based on [101, 108, 109, 112].

The BED model algorithm that was selected is the standard one of the first generation. For hyperfractionation as a first step research choice [25, 83]. The numerical difference has not been checked implementing further generations of BED algorithms. However, as a tentative calculus given the numerical data obtained, it seems that the numerical differences could not differ significantly from the first generation model function. The L_1 norm selected (Tikhonov L_1 norm) was applied for programming simplification. In previous articles, it was found that software implementation of (Tikhonov L_2) norm did not show substantial differences with L_1 norm. Besides, the design of the program for L_2 norm results be more complicated and does not bring important variances. Other featureis that the implementation of the L_2 norm implies a longer running time, which is an added difficulty. First simulation shows higher number of fractions, and lower magnitude of dose per fraction than the second simulation, Tables 5-6.

Factually, and according to recent literature [101-109], GA-PMO method is more widely used compared to Inverse Optimization with Least Squares algorithm, for example, [11-16]. Recent optimization methods tend to apply/use more frequently evolutionary algorithms and also the variants and improved GA algorithms based on successive method-generations.

3D-imaging Interior Optimization (the basic) was implemented, e. g., for superconductors modelling with acceptable numerical results in a series of publications, for example [110]. Although 3D-IO technique is essentially a numerical imaging-processing one, the 2D GA-PMO method gives also acceptable information and dataset for the approached problem.

The software that was designed for the research is based on previous studies for applications of GA standard method, e. g., [110]. The implemented dataset is founded on the lung cancer current protocol doses and do not differ in magnitude order along the literature. As an example, these calculations boundaries and magnitude orders were modernly confirmed in [111]. Therefore, the constraints and boundaries set in programming patterns can be considered acceptable.

In terms of programming running time, it was checked that the approximate average time to obtain a simple GA chart was about 2 minutes, provided that number of generations not be higher than [200, 300]. If the generations number increases from 150, approximately, the running time could reach 3 or 4 minutes. The Multigraphics take an average of 2 minutes more than the simple ones.

The numerical data obtained matches the average literature dataset [99-111], with very low differences. Specially the recent protocols in Radiosurgery [100], coincide with the dosimetry results. When numer of generations is increased, no significant changes are observed in magnitude orders for Pareto 1 and 2 Multiobjective Functions.

The objective of the study was not discussed between hyperfractionation versus hypofractionation. However, according to results it si possible to comment some classical ideas about this controversial matter. There are Hyperfractionation, Hypofractionation, Hybrid Schedule and Accelerated Hyperfractionation dose delivery schedules. Hospital institutions differ in technical facilities, staff specialization, and treatment time available, therefore this question adds another influential factor for those optimal clinical-radiation oncology decisions.

Author's criterion is that all of them should be treated/considered in function of personalized RT treatment, and the most important idea is that all of them depend on multiple factors [22-25, 87-89,91]. one important factor is the magnitude order of the coefficients alpha and betha for tumoral tissue at every patient, if time and hospital facilities can determine those.

Hyperfractionation considers that the higher recovery capacity of late-responding normal tissues, in practical terms NTCP magnitude, is higher when contrasted with tumour-tissue. If the response of normal tissues is low, it implies that the quotient (alpha/betha) has a lower magnitude order). However, the more fractions get the schedule, the higher changes of this quotient is observed. For comparative considerations between Hyper and Hypofractionation. The dose difference between the plottings of TCP versus dose fraction magnitude gives essential information for selecting options in dose delivery schedule.

The PMO-BED model image processing results are sharp in several imaging formats, from simple 2D graphics to multifunctional ones. These series of results can be considered acceptable, Figures 1-9, Tables 3-4. Two simulations were presented as objective of the research, computationally designed for head and neck tumors [82-88]. It was intended to set in software precise experimental constants [22,81-88]. Therefore, 3D simulations could offer a realistic graphical and numerical dataset this type of cancers. Two different simulations with different constraints are shown and proven. Currently, biological models get a rationale experimental proven through radiobiology studies [76-80]. TCP and NTCP constitute acceptable parameters to predict patient survival time [20, 87-88, 111].

The method main advantages are graphics sharpness, low numerical residuals, demonstration of operability of this modern AI method, and contrast between two different BED criteria parameters. Inconvenients are that in literature experimental data parameters differ numerically [87-88, 91]. The algorithm is based on the simplest BED model [22-25] at this stage. Running time is rather longer compared to Inverse Least Squares Optimization [1-21].

Grosso modo, Pareto Multiobjective BED model was got for applied for optimization of radiotherapy BED algorithm in Lung cancer. The practical radiotherapy physics significance is an improved radiation therapy treatment for these tumors RT medical physics computational planning.

SCIENTIFIC ETHICS STANDARDS

This article shows additional results that complement previous studies and contributions, recently [87-88]. All the images are new/improved and numerical results from former publications are extended and detailed. GA Artificial Intelligence software was developed originally by Dr Casesnoves on September 2022. Figures 8-9 are new but developed from software in [87,88,91]. All initial modelling equations were developed from previous researchers contributions [1-25,87-88]. This article has previous papers mathematical techniques, reviews with explanations, [1-21, 75], whose use was

essential to make model numerical solutions and approximations. The number of Dr Casesnoves publications at references is intended also for reader's learning and consultation. This study was carried out, and their contents are done according to the European Union Technology and Science Ethics and International Scientific Ethics norms [38,43-45]. This research was completely done by the author, the calculations, images, mathematical propositions and statements, reference citations, and text is original from the author. When a mathematical statement, proposition or theorem is presented, demonstration is always included. If any results inconsistency is found after publication, it is clarified in subsequent contributions. When a citation such as [Casesnoves, 'year'] appears, there is not vanity or intention to brag. The reason is to keep clearly the intellectual property. The article is exclusively scientific, without any commercial, institutional, academic, religious, religious-similar, non-scientific theories, personal opinions, friends and/or relatives favours, political ideas, or economical influences. When anything is taken from a source, it is adequately recognized. Ideas and some text expressions/sentences from previous publications were emphasized due to a clarification aim [38,43-45].

SOME RECENT AUTHOR'S RADIOTHERAPY REFERENCES

1. Casesnoves, F; (2024). Advanced Radiotherapy 3d Isodosezones Optimization for Hyperfractionated Treatment Planning Optimization in Lung Tumors with Repair-Tissue Factors Mathematical Review. Int. j. adv. multidisc. res. Stud. 2024; 4(6):553-563. 2024.
2. Casesnoves, F; (2024). Radiotherapy 3D Isodosezones Graphical Optimization for Hyperfractionated Treatment Planning in Lung and Prostate Tumors with Bed Pareto-Multiobjective Model Dataset. Int J Sci Res Sci & Technol. July-August-2024, 11 (4): 89-103. 2024.
3. Casesnoves, F; (2023). Radiotherapy Genetic Algorithm Pareto-Multiobjective Optimization of Biological Effective Dose and Clonogens Models for Breast Tumor Improved Treatment. International Journal of Mathematics and Computer Research ISSN: 2320-7167. Volume 11 Issue 01 January 2023, Page no. – 3102-3114 Index Copernicus ICV: 57.55, Impact Factor: 7.362. DOI: 10.47191/ijmcr/v11i1.02. 2023.
4. Casesnoves, F; (2024). Radiotherapy 3D Isodosezones Graphical Optimization for Hyperfractionated Treatment Planning Dosimetry in Lung and Head-Neck Tumors with Biological Effective Dose Model. International Journal of Mathematics and Computer Research. ISSN: 2320-7167 Volume 12 Issue 06 June 2024, Page no. – 4323-4336. Index Copernicus ICV: 57.55, Impact Factor: 8.316. DOI: 10.47191/ijmcr/v12i6.12. 2024.

REFERENCES

1. Casesnoves F (2022). Radiotherapy Wedge Filter AAA Model 18 MeV Dose Delivery 3D Simulations with Several Software Systems for Medical Physics Applications. Applications. Biomed J Sci & Tech Res 40(5). DOI: 10.26717/BJSTR.2022.46.007337.
2. Casesnoves F (2016). Mathematical Exact 3D Integral Equation Determination for Radiotherapy Wedge Filter Convolution Factor with Algorithms and Numerical Simulations.Journal of Numerical Analysis and Applied Mathematics 1(2): 39-59. ISSN Online: 2381-7704.
3. Casesnoves F (2015). Radiotherapy Conformal Wedge Computational Simulations,Optimization Algorithms, and Exact Limit Angle Approach. International Journal of Scientific Research in Science, Engineering and Technology (IJSRSET) 1(2): 353-362. Print ISSN: 2395-1990. Online ISSN: 2394-4099.
4. Casesnoves F (2019). Improvements in Simulations for Radiotherapy Wedge Filter dose and AAA-Convolution Factor Algorithms. International Journal of Scientific Research in Science, Engineering and Technology (IJSRSET) 6(4): 194-219. Print ISSN: 2395-1990. Online ISSN: 2394-4099.
5. Casesnoves F (2011). Exact/Approximated Geometrical Determinations of IMRT Photon Pencil-Beam Path Through Alloy Static Wedges in Radiotherapy Using Anisothropic Analytic Algorithm (AAA). Peer-reviewed ASME Conference Paper. ASME 2011 International Mechanical Eng Congress. Denver. USA. IMECE2011-65435.
6. Casesnoves F (2012). Geometrical Determinations of Limit angle (LA) related to maximum Pencil-Beam Divergence Angle in Radiotherapy Wedges. Peer-reviewed ASME Conference Paper. ASME 2012 International Mechanical Eng Congress. Houston. USA. IMECE2012-86638.
7. Casesnoves F (2013). A Conformal Radiotherapy Wedge Filter Design. Computational and Mathematical Model/Simulation'. Peer-Reviewed Poster IEEE (Institute for Electrical and Electronics Engineers), Northeast Bioengineering Conference. Syracuse New York, USA. April 6th, 2013. Peer-Reviewed Poster Session on 6th April 2013. Sessions 1 and 3 with Poster Number 35. Page 15 of Conference Booklet Printed.
8. Casesnoves F (2014). Mathematical and Geometrical Formulation/Analysis for Beam Limit Divergence Angle in Radiotherapy Wedges. Peer-Reviewed International Engineering Article. International Journal of Engineering and Innovative Technology (IJEIT). 3(7). ISSN: 2277-3754. ISO 9001:2008 Certified.
9. Casesnoves F (2014). Geometrical determinations of IMRT photon pencil-beam path in radiotherapy wedges and limit divergence angle with the Anisotropic Analytic Algorithm (AAA) Casesnoves, F. Peer- Reviewed scientific paper, both Print and online. International Journal of Cancer Therapy and Oncology 2 (3): 02031. DOI:10.14319/IJCTO.0203.1. Corpus ID: 460308.

10. Casesnoves F (2014). Radiotherapy Conformal Wedge Computational Simulations and Nonlinear Optimization Algorithms. Peer-reviewed Article, Special Double-Blind Peer-reviewed paper by International Scientific Board with contributed talk. Official Proceedings of Bio- and Medical Informatics and Cybernetics: BMIC 2014 in the context of the 18th Multi-conference on Systemics, Cybernetics and Informatics: WMSCI 2014 July 15 - 18, 2014, Orlando, Florida, USA. ISBN: 978-1-941763-03-2 (Collection). ISBN: 978-1-941763-10-0 (Volume II).
11. Casesnoves F (2007). Large-Scale Matlab Optimization Toolbox (MOT) Computing Methods in Radiotherapy Inverse Treatment Planning'. High Performance Computing Meeting. Nottingham University. Conference Poster.
12. Casesnoves F (2008). A Computational Radiotherapy Optimization Method for Inverse Planning with Static Wedges. High Performance Computing Conference. Nottingham University. Conference Poster.
13. Casesnoves F (2015). Radiotherapy Conformal Wedge Computational Simulations, Optimization Algorithms, and Exact Limit Angle Approach. International Journal of Scientific Research in Science, Engineering and Technology 1(2). Print ISSN: 2395-1990, Online ISSN: 2394-4099.
14. Casesnoves F (2015). Radiotherapy Standard/Conformal Wedge IMRT-Beamlet Divergence Angle Limit Exact Method, Mathematical Formulation, and Bioengineering Applications. International Article-Poster. Published in Proceedings of Conference. 41st Annual Northeast Bioengineering Conference. Rensselaer Polytechnic Institute. Troy, New York USA, April, p. 17-19. DOI:10.1109/NEBEC.2015.7117152. Corpus ID: 30285689.
15. Casesnoves F (2015). Radiotherapy Standard/Conformal Wedge IMRT-Beamlet Divergence Angle Limit Exact Method, Mathematical Formulation, and Bioengineering Applications. IEEE (Institute for Electrical and Electronics Engineers), International Article-Poster. http://ieeexplore.ieee.org/stamp/stamp.jsp?tp=&arnumber=7117152.
16. Casesnoves F (2015). Abstract-Journal. 'Radiotherapy Standard/ Conformal Wedge IMRT-Beamlet Divergence Angle Limit Exact Method, Mathematical Formulation. International Conference on Significant Advances in Biomedical Engineering. 252nd OMICS International Conference 5(1). Francisco Casesnoves, J Bioengineer & Biomedical Sci 2015, 5:1. http://dx.doi.org/10.4172/2155-9538.S1.003.
17. Casesnoves, F (2001). Determination of absorbed doses in common radio diagnostic explorations. 5th National Meeting of Medical Physics. Madrid, Spain. September 1985. treatment Planning'.
18. Casesnoves, F (2001). Master Thesis in Medical Physics. Eastern Finland University. Radiotherapy Department of Kuopio University Hospital and Radiotherapy Physics University-Kuopio. Defense approved in 2001. Library of Eastern Finland University. Finland.
19. Casesnoves F (2013). A Conformal Radiotherapy Wedge Filter Design. Computational and Mathematical Model/Simulation'. Peer-Reviewed Poster IEEE (Institute for Electrical and Electronics Engineers), Northeast Bioengineering Conference. Syracuse New York, USA. Presented in the Peer-Reviewed Poster Session on 6th April 2013. Sessions 1 and 3 with Poster Number 35. Page 15 of Conference Booklet. April 6th, 2013.
20. Casesnoves F (2022). Radiotherapy Biological Tumor Control Probability Integral Equation Model with Analytic Determination. International Journal of Mathematics and Computer Research 10(8): 2840-2846. DOI: https://doi.org/10.47191/ijmcr/v10i10.01.
21. Casesnoves F (2022). Radiotherapy Wedge Filter AAA Model 3D Simulations For 18 Mev 5 cm-Depth Dose with Medical Physics Applications", International Journal of Scientific Research in Computer Science, Engineering and Information Technology (IJSRCSEIT) 8(1): 261-274. ISSN: 2456-3307 (www.ijsrcseit.com). DOI: https://doi.org/10.32628/CSEIT228141.
22. Walsh S (2011). Radiobiological modelling in Radiation Oncology. PhD Thesis. School of Physics. National University of Galway. http://hdl.handle.net/10379/3027.
23. Chapman D, Nahum, A (2015). Radiotherapy Treatment Planning, Linear- Quadratic Radiobiology. CRC Press. ISBN 9780367866433.
24. Mayles, W, Nahum A (2015). Rosenwald, J. Editors. Handbook of Radiotherapy Physics. Second Edition. CRC Press. ISBN 9780367192075. International Standard Book Number-13: 978-1-4987-2146-2.
25. Nahum, A, Webb, S (1993). A model for calculating tumour control probability in radiotherapy including the effects of inhomogeneous distributions of dose and clonogenic cell density. Physics in Medicine and Biology; v. 38(6); p. 653-666. ISSN 0031-9155.
26. Haydaroglu, A, Ozyigit G (2013). Principles and Practice of Modern Radiotherapy Techniques in Breast Cancer. Springer. DOI:10.1007/978-1-4614-5116-7.
27. Casesnoves, F (2019-20). Die numerische Reuleaux-Methode Rechnerische und dynamische Grundlagen mit Anwendungen (Erster Teil). ISBN-13: 978-620-0-89560-8, ISBN-10: 6200895600. Publishing House: Sciencia Scripts. 2019-20.
28. Ulmer W, Harder, D (1997). Corrected Tables of the Area Integral I(z) for the Triple Gaussian Pencil Beam Model. Z Med Phys 7: 192-193. DOI: https://doi.org/10.1016/S0939-3889(15)70255-2.
29. Ulmer W, Harder, D (1995) A triple Gaussian pencil beam model for photon beam treatment planning. Med. Phys 5: 25-30. DOI :10.1016/S0939-3889(15)70758-0.
30. Ulmer W, Harder D (1996). Applications of a triple Gaussian pencil beam model for photon beam treatment planning. Med Phys 6: 68-74. https://doi.org/10.1016/S0939-3889(15)70784-1.
31. Ma, C, Lomax, T (2013). Proton and Carbon Ion Therapy. CRC Press. DOI: https://doi.org/10.1201/b13070.

32. Censor, Y, Zenios, S (1997). Parallel Optimization: Theory, Algorithms and Applications'. UOP. DOI:10.12694/SCPE.V3I4.207. Corpus ID: 19584334.
33. Ulmer, W, Pyyry, J, Kaissl, W (2005). A 3D photon superposition/ convolution algorithm and its foundation on results of Monte Carlo calculations. Phys Med Biol, p. 50. DOI: 10.1088/0031-9155/50/8/010.
34. Ulmer, W, Harder, D (1997). Applications of the triple Gaussian Photon Pencil Beam Model to irregular Fields, dynamical Collimators and circular Fields. Phys Med Biol. DOI: https://doi.org/10.1023/B:JORA.0000015192.56164.a5.
35. Haddad K, Anjak O, Yousef B (2019). Neutron and high energy photon fluence estimation in CLINAC using gold activation foils. Reports of practical oncology and radiotherapy 24: 41-46. DOI: 10.1016/j.rpor.2018.08.009.
36. Sievinen J, Waldemar U, Kaissl W. AAA Photon Dose Calculation Model in Eclipse™. Varian Medical Systems Report. Rad #7170A.
37. Vagena E, Stoulos S, Manolopoulou M (2016). GEANT4 Simulations on Medical LINAC operation at 18MV: experimental validation based on activation foils. Radiation Physics and Chemistry. DOI: 10.1016/j.radphyschem.2015.11.030.
38. Ethics for Researchers (2013). EU Commission. Directorate-General for Research and Innovation. Science in society/Capacities FP7. https://data.europa.eu/doi/10.2777/7491.
39. Casesnoves F (1981). Surgical Pathology I course class notes and clinical practice of Surgical Pathology Madrid Clinical Hospital [Professor Surgeon Dr Santiago Tamames Escobar]. 4th academic year course for graduation in Medicine and Surgery. Lessons and practice Lung Cancer Surgical and Medical Treatment. 1980-1981. Madrid Complutense University.
40. Tamames Escobar, S (2000). Cirugia/ Surgery: Aparato Digestivo. Aparato Circulatorio. Aparato Respiratorio/ Digestive System. Circulatory System. Respiratory System (Spanish Edition). ISBN 10: 8479034955. ISBN 13: 9788479034955.
41. Silvia C Formenti, Sandra Demaria (2013). Combining Radiotherapy and Cancer Immunotherapy: A Paradigm Shift Silvia C. Formenti, Sandra Demaria. J Natl Cancer Inst 105: 256-265. DOI: 10.1093/jnci/djs629.
42. Numrich R, (2010). The computational energy spectrum of a program as it executes. Journal of Supercomputing 52. DOI:10.1007/s11227-009-0273-x.
43. European Commission, Directorate-General for Research (2021). Unit L3. Governance and Ethics. European Research Area. Science and Society.
44. ALLEA (2017). The European Code of Conduct for Research Integrity, Revised Edn.; ALLEA: Berlin Barndenburg Academy of Sciences.
45. Good Research Practice (2017) Swedish Research Council. ISBN 978-91- 7307-354-7.
46. Ulmer W, Schaffner, B (2011). Foundation of an analytical proton beamlet model for inclusion in a general proton dose calculation system. Radiation Physics and Chemistry 80: 378-389. DOI: 10.1016/j.radphyschem.2010.10.006.
47. Sharma, S (2008). Beam Modification Devices in Radiotherapy. Lecture at Radiotherapy Department, PGIMER. India.
48. Barrett, A, Colls (2009). Practical Radiotherapy Planning. Fourth Edition. Hodder Arnold. ISBN 9780340927731.
49. Ahnesjö A, Saxner M, A Trepp (1992). A pencil beam model for photon dose calculations. Med Phys, pp. 263- 273. DOI:10.1118/1.596856.
50. Brahime A (2000). Development of Radiation Therapy Optimization. Acta Oncologica 39(5). DOI: 10.1080/028418600750013267.
51. Bortfeld T, Hong T, Craft D, Carlsson F (2008). Multicriteria Optimization in Intensity-Modulated Radiation Therapy Treatment Planning for Locally Advanced Cancer of the Pancreatic Head. International Journal of Radiation Oncology and Biology Physics 72(4). DOI: 10.1016/j.ijrobp.2008.07.015.
52. Brown, B, and cols (2014). Clinician-led improvement in cancer care (CLICC)-testing a multifaceted implementation strategy to increase evidence-based prostate cancer care: phased randomised controlled trial - study protocol. Implementation Science 9: 64. DOI: https://doi.org/10.1186/1748-5908-9-64 .
53. Bortifield, T (2006). IMRT: a review and preview. Phys Med Biol 51(2006): R363–R379. DOI: 10.1088/0031-9155/51/13/R21.
54. Censor, Y (1996). Mathematical Optimization for the Inverse problem of Intensity-Modulated Radiation Therapy. Laboratory Report, Department of Mathematics, University of Haifa, Israel.
55. Capizzello A, Tsekeris PG, Pakos EE, Papathanasopoulou V, Pitouli EJ (2006). 'Adjuvant Chemo-Radiotherapy in Patients with Gastric Cancer. Indian Journal of Cancer 43(4). ISSN: 019-509X.
56. Tamer Dawod, EM Abdelrazek, Mostafa Elnaggar, Rehab Omar (2014). Dose Validation of Physical Wedged symmetric Fields in Artiste Linear Accelerator. International Journal of Medical Physics, Clinical Engineering and Radiation Oncology 3: 201-209. DOI: 10.4236/ijmpcero.2014.34026.
57. Do SY, David A, Bush Jerry D Slater (2010). Comorbidity-Adjusted Survival in Early-Stage Lung Cancer Patients Treated with Hypofractioned Proton Therapy. Journal of Oncology. DOI: 10.1155/2010/251208.
58. Ehrgott M, Burjony M. (1999). Radiation Therapy Planning by Multicriteria Optimization. Department of Engineering Science. University of Auckland. New Zealand. Conference Paper.

59. Ezzel, G (1996). Genetic and geometric optimization of three-dimensional radiation therapy treatment planning. Med Phys 23: 293- 305. DOI: 10.1118/1.597660.
60. Effective Health Care, (2008). Number 13. Comparative Efectiveness of Therapies for Clinically Localized Prostate cancer. Bookshelf ID: NBK554842.
61. Hansen, P (1998). Rank-deficient and discrete ill-posed problems: numerical aspects of linear inversion'. SIAM monographs on mathematical modelling and computation. ISBN-13: 978-0898714036.
62. Hashemiparast, S, Fallahgoul H (2011). Modified Gauss quadrature for ill-posed integral transform. International Journal of Mathematics and Computation 13(11). ISSN: 0974-570X.
63. Isa, N (2014). Evidence based radiation oncology with existing technology. Reports of practical oncology and radiotherapy 19: 259-266. DOI: 10.1016/j.rpor.2013.09.002
64. Johansson KA, Mattsson S, Brahme A, Turesson I (2003) Radiation Therapy Dose Delivery. Acta Oncologica 42(2): 2003. DOI :10.1080/02841860310004922.
65. Khanna P, Blais N, Gaudreau PO, Corrales-Rodriguez L (2016). Immunotherapy Comes of Age in Lung Cancer, Clinical Lung Cancer. DOI: 10.1016/j.cllc.2016.06.006.
66. Kufer KH, Hamacher HW, Bortfeld T (2000). A multicriteria optimisation approach for inverse radiotherapy planning. University of Kaiserslautern, Germany. DOI: 10.1007/978-3-642-59758-9_10.
67. Kirsch A (1996). An introduction to the Mathematical Theory of Inverse Problems. Springer Applied Mathematical Sciences. Series E-ISSN2196-968X.
68. Luenberger, D (1989). Linear and Nonlinear Programming (2nd Edn.). Addison-Wesley. ISBN-13: 978-3030854492.
69. Moczko, J, Roszak, A (2006). Application of Mathematical Modeling in Survival Time Prediction for Females with Advanced Cervical cancer treated Radio-chemotherapy. Computational Methods in science and Technology 12(2). DOI: 10.12921/cmst.2006.12.02.143-147
70. Ragaz, J, Ivo A Olivotto, John J Spinelli, Norman Phillips, Stewart M Jackson, et al. (2005). Regional Radiation Therapy in Patients with High-risk Breast Cancer Receiving Adjuvant Chemotherapy: 20-Year Results of the Columbia Randomized Trial'. Journal of National Cancer Institute 97(2). DOI: 10.1093/jnci/djh297.
71. Steuer R (1986). Multiple Criteria Optimization: Theory, Computation and Application. Wiley. https://doi.org/10.1002/oca.4660100109.
72. Spirou SV, Chui CS (1998). A gradient inverse planning algorithm with dose-volume constraints. Med Phys 25: 321-323. DOI: 10.1118/1.598202.
73. Das I, and colls (1997). Patterns of dose variability in radiation prescription of breast cancer. Radiotherapy and Oncology 44: 83-89. DOI: 10.1016/s0167-8140(97)00054-6
74. Casesnoves, F (2018). Practical Radiotherapy TPO course and practice with Cyberknife. Robotic simulations for breathing movements during radiotherapy treatment. Sigulda Radiotherapy Cyberknife Center. Latvia. Riga National Health Oncology Hospital Varian LINACs TPO practice/lessons several Varian LINACs. Riga Technical University Bioengineering Training-Course Nonlinear Life. August 2018.
75. Casesnoves, F. (2022). Radiotherapy Linear Quadratic Bio Model 3D Wedge Filter Dose Simulations for AAA Photon-Model [18 Mev, Z= 5,15 cm] with Mathematical Method System. Biomed J Sci & Tech Res 46(2)-2022. BJSTR. MS.ID.007337. DOI: 10.26717/BJSTR.2022.46.007337.
76. Casesnoves, F (1985). Master in Philosophy Thesis at Medical Physics Department. Protection of the Patient in Routinary Radiological Explorations. Experimental Low Energies RX Dosimetry. Medicine Faculty. Madrid Complutense University. 1984-85.
77. Casesnoves, F (1983-5). Ionization Chamber Low Energies Experimental Measurements for M-640 General Electric RX Tube with Radcheck ionization camera, Radcheck Beam Kilovoltimeter and TLD dosimeters. Radiology Department practice and measurements. Madrid Central Defense Hospital. Medical Physics Department. Master in Philosophy Thesis. Medicine Faculty. Complutense University. Madrid.
78. Casesnoves, F (1985). Determination of Absorbed Doses in Routinary Radiological Explorations. Medical Physics Conference organized by Medical Physics Society Proceedings Printed. San Lorenzo del Escorial. Madrid. September 1985.
79. Greening, J (1985). Fundamentals of Radiation Dosimetry. Taylor and Francis. Second Edition. 1985. DOI: https://doi.org/10.1201/9780203755198.
80. International Commission of Radiation Protection (1977). Bulletin 26th. The International Commission on Radiological Protection. Recommendations of the International Commission on Radiological Protection. Pergamon Press. Copyright © 1977 The International Commission on Radiological Protection.
81. Stanton, P; Colls (1996). Cell kinetics in vivo of human breast cancer. British Journal of Surgery 1996,83,98-102. DOI: https://doi.org/10.1002/bjs.1800830130 .
82. Hedman M, Bjork-Eriksson T, Brodin O, Toma-Dasu I (2013). Predictive value of modelled tumour control probability based on individual measurements of in vitro radiosensitivity and potential doubling time. Br J Radiol 2013;86: 20130015. DOI:10.1259/bjr.20130015.
83. Fowler, J. 21 years of Biologically Effective Dose.The British Journal of Radiology, 83 (2010), 554–568.

84. Marcu, L, and al. Radiotherapy and Clinical Radiobiology of Head and Neck Cancer. Series in Medical Physics and Biomedical Engineering. CRC Press. 2018.
85. Casesnoves, F. Radiotherapy 3D Isodose Simulations for Wedge Filter 18 Mev-Dose [z = 5,15 cm] with AAA Model with Breast Cancer Applications. International Journal on Research Methodologies in Physics and Chemistry (IJRPC) ISSN: 2349-7963 Volume: 9 Issue: 2. 2022.
86. Garden, A; Beadle, B; Gunn, G. Radiotherapy for Head and Neck Cancers. Fifth Edition. Wolters Kluwer. 2018.
87. Casesnoves, F. Radiotherapy Genetic Algorithm Pareto-Multiobjective Optimization of Biological Efective Dose and Clonogens Models for Head and Neck Tumor Advanced Treatment. International Journal of Mathematics and Computer Research. ISSN: 2320-7167. Volume 11 Issue 01 January 2023, Page no. – 3156-3177. DOI: 10.47191/ijmcr/v11i1.08.
88. Casesnoves, F. Radiotherapy effective clonogens model graphical optimization approaching linear quadratic method for head and neck tumors. International Journal of Molecular Biology and Biochemistry. ISSN Print: 2664-6501. ISSN Online: 2664-651X. Impact Factor: RJIF 5.4. IJMBB 2023; 5(1): 33-40.
89. Lindblom, E; Dasu A; Iuliana Toma-Dasu, I. (2015). Optimal fractionation in radiotherapy for non-small cell lung cancer – a modelling approach, Acta Oncologica, 54:9, 1592-1598, DOI: 10.3109/0284186X.2015.1061207 .
90. Kaidar-Person, O; Chen, R. (2018). Hypofractionated and Stereotactic Radiation Therapy. Springer. ISBN 978-3-319-92800-5 ISBN 978-3-319-92802-9 (eBook). https://doi.org/10.1007/978-3-319-92802-9 .
91. Casesnoves, F. (2022). Radiotherapy Genetic Algorithm Pareto-Multiobjective Optimization of Biological Effective Dose and Clonogens Models for Breast Tumor Improved Treatment. International Journal of Mathematics and Computer Research ISSN: 2320-7167. Volume 11 Issue 01 January 2023, Page no. – 3102-3112. Index Copernicus ICV: 57.55, Impact Factor: 7.362. DOI: 10.47191/ijmcr/v11i1.02.
92. Wong, J; Schultheiss, T; Radany, E (2017). Advances in Radiation Oncology. Springer. DOI 10.1007/978-3-319-53235-6.
93. Huo, M; Gorayski, P; Pinkham, M; Lehman, M. (2016). AFP VOL.45, No.11, November 2016. Australian College of General Practitioners 2016.
94. College of Radiologists UK. (2019). Radiotherapy dose fractionation. Third edition. Clinical Oncology. www.rcr.ac.uk. 2019.
95. Murshed, M. (2019). Fundamentals of radiation oncology physical, biological, and clinical aspects. Academic Press. Elsevier.
96. Hedin, E. (2016). Estimation of clinical dose distributions for breast and lung cancer radiotherapy treatments. PhD thesis. Gothenburg University.
97. Reckamp, K (2016). Lung cancer, treatment and research. Springer. ISSN 0927-3042. ISBN 978-3-319-40387-8. DOI 10.1007/978-3-319-40389-2. 2016.
98. Casesnoves, F. Radiotherapy Genetic Algorithm Pareto-Multiobjective Optimization of Biological Efective Dose and Clonogens Models for Head and Neck Tumor Advanced Treatment. International Journal of Mathematics and Computer Research. ISSN: 2320-7167. Volume 11 Issue 01 January 2023, Page no. – 3156-3177. DOI: 10.47191/ijmcr/v11i1.08.
99. Casesnoves, F. Radiotherapy effective clonogens model graphical optimization approaching linear quadratic method for head and neck tumors. International Journal of Molecular Biology and Biochemistry. ISSN Print: 2664-6501. ISSN Online: 2664-651X. Impact Factor: RJIF 5.4. IJMBB 2023; 5(1): 33-40.
100. Casesnoves, F (2023). Training course Stereotactic Radiotherapy and Radiosurgery in Management of Metastatic Brain Tumors. Sigulda Stereotactic, Radiosurgery and Cyberknife Hospital. International Society of Radiosurgey. Sigulda, Latvia. June 2023.
101. Joiner, M; Kogel, A (2019). Basic Clinical Radiobiology. ISBN 9781444179637. CRC Press.
102. Cher, M; Raz, A (2002). Prostate Cancer: New Horizons in Research and Treatment. Print ISBN: 1-4020-7352-6. Kluwer Academic Publishers. 2002.
103. Sureka, C; Armpilia, C (2017). Radiation Biology for Medical Physicists. ISBN-13: 978-1-4987-6589-3 (Hardback). CRC Press. 2017.
104. Andisheh, B; Edgren, M; Belkić, D; Mavroidis, P; Brahme, A (2013). A Comparative Analysis of Radiobiological Models for Cell Surviving Fractions at High Doses. Technology in Cancer Research and Treatment 12(2):183-192.
105. Casesnoves, F (2023). Radiotherapy BED Model 2D Pareto- Multiobjective Evolutionary Optimization for Prostate Cancer Hyperfractionated Treatment. Biomed J Sci & Tech Res 51(2)-2023. BJSTR. MS.ID.008064.
106. Borst, G. Radiotherapy for Lung Cancer (2009). ISBN/EAN: 978-90-9024742-7. Printed by: Ipskamp Drukkers. Gerben Borst, Amsterdam 2009.
107. Trombetta, M, et alter (2018). Alternate Fractionation in Radiotherapy. Springer. ISBN 978-3-319-51197-9 ISBN 978-3-319-51198-6. 2018.
108. Reckamp, K (2016). Lung cancer, treatment and research. Springer. ISSN 0927-3042. ISBN 978-3-319-40387-8. DOI 10.1007/978-3-319-40389-2. 2016.
109. Altmann, K; Lett, J. (1992). Advances in radiation biology. Relative Radiation Sensitivities of Human Organ Systems, Part III. Academic Press.

110. Casesnoves, F. Genetic Algorithms for Interior Comparative Optimization of Standard BCS Parameters in Selected Superconductors and High-Temperature Superconductors. Standards 2022, 2, 430–448. https://doi.org/10.3390/standards2030029.
111. Casesnoves, F (2023). Training course Stereotactic Radiotherapy and Radiosurgery in Management of Metastatic Brain Tumors. Sigulda Stereotactic, Radiosurgery and Cyberknife Hospital. International Society of Radiosurgey. Sigulda, Latvia. June 2023.
112. Carini, H; Fidock, M; Van Gooland, A (2019). Handbook of Biomarkers and Precision Medicine. CRC Press. ISBN-13: 978-1-4987-6258-89. 2019.

CITATION
Casesnoves F. (2025). Radiotherapy Lung Cancer Advanced Treatment Planning Optimization for Fractionated Biological Effective Dose with Genetic Algorithm Pareto-Multiobjective Method. Third Part. In Global Journal of Research in Engineering & Computer Sciences (Vol. 5, Number 4, pp. 51–79).
https://doi.org/10.5281/zenodo.16938699

AUTHOR'S BIOGRAPHY

Dr Francisco Casesnoves earned the Engineering and Natural Sciences PhD by Talllinn University of Technology (started thesis in 2016, thesis Defence/PhD earned in December 2018, official graduate Diploma 2019). He works as independent research scientist in computational-engineering/physics, and actually is Director of Independent Bioengineering Laboratory. Dr Casesnoves earned MSc-BSc, Physics/Applied-Mathematics (Public Eastern-Finland-University, MSc Thesis in Radiotherapy Treatment Planning Optimization, which was developed after graduation in a series of Radiation Therapy Optimization-Modelling publications [2007-present]). Dr Casesnoves earned Graduate-with-MPhil, in Medicine and Surgery [1983] (Madrid University Medicine School, MPhil in Radioprotection Low Energies Dosimetry [1985]). Casesnoves resigned definitely to his original nationality in 2020 for ideological reasons, anti-monarchy-corruption, democratic-republican ideology, and ethical-professional reasons, and does not belong to Spain Kingdom anymore. His constant service to the International Scientific Community and Estonia Republic technological progress involves about 100 DOI articles, more than 120 total publications, and about 4 books. Recent advances published are in Superconductors Mathematical Modelling and Radiotherapy Brain Neurobiological Models, 3D-AI Isodosezones and Isodoselines. Among Dr. Casesnoves inventions and scientific creations are:

1. Numerical Reuleaux Method.
2. Radiotherapy Omega Factor correction for AAA model wedge filters dose delivery.
3. Integral-Differential materials erosion model.
4. Graphical Optimization.
5. Interior Optimization Methods.
6. Superconductors Molecular Effect Model.
7. Superconductors Multifunctional Transmission Line.
8. BED radiotherapy model GA and Graphical Optimization Isodoselines and Isodosezones.
9. Aerospace Turbulence Energy Absorbing System